



**Fermi National Accelerator Laboratory**

**FERMILAB-Conf-92/79  
E731**

**Latest Results on the Direct  
CP Violation Measurements -  $\epsilon'/\epsilon$**

**Y. Hsiung  
(E731 Collaboration)**

*Fermi National Accelerator Laboratory  
P.O. Box 500, Batavia, Illinois 60510*

**March 1992**

**Talk given at the 1991 SLAC Summer Institute, Topical Conference, SLAC, Stanford, California,  
August 14-16, 1991.**



**LATEST RESULTS ON THE DIRECT CP VIOLATION  
MEASUREMENTS –  $\epsilon'/\epsilon$  §**

Yee B. Hsiung  
(E731 collaboration)  
*Fermi National Accelerator Laboratory, P. O. Box 500  
Batavia, Illinois 60510, U.S.A.*

March 1992

---

§ Talk given at the 1991 *SLAC Summer Institute, Topical Conference*, SLAC, Stanford, California, August 14-16, 1991.

# LATEST RESULTS ON THE DIRECT CP VIOLATION MEASUREMENTS - $\epsilon'/\epsilon$

Yee B. Hsiung  
(E731 collaboration)  
*Fermi National Accelerator Laboratory, P. O. Box 500  
Batavia, Illinois 60510, U.S.A.*

## ABSTRACT

Preliminary results, based on the full data sample from Fermilab-E731 and the combined data sample from CERN-NA31, on the "direct" CP-violation measurements  $\epsilon'/\epsilon$  in neutral kaon decay have been reviewed. The E731's result is  $Re(\epsilon'/\epsilon) = (6.0 \pm 5.8(\text{stat}) \pm 3.2(\text{syst}) \pm 1.8(\text{MC})) \times 10^{-4}$ , which provides no evidence for "direct" CP-violation, thus supporting the Superweak model; while the NA31's combined result ('86+'88+'89 data) is  $Re(\epsilon'/\epsilon) = (23 \pm 3.4(\text{stat}) \pm 6.5(\text{syst})) \times 10^{-4}$ , three standard deviations from zero, which provides evidence for the "direct" CP-violation in the Standard Model. Comparisons of the two experiments are made. The Fermilab-E731 group has also fit for the other parameters of the neutral kaon system in their  $2\pi$  data sample, such as: the  $K_S$  life time  $\tau_S$ ; the  $K_L$ - $K_S$  mass difference  $\Delta m$ ; the phase difference between  $\eta_{00}$  and  $\eta_{+-}$ ,  $\Delta\phi = (-0.6 \pm 1.6)^\circ$ , which is a test of CPT invariance; the Superweak phase  $\phi_{SW} = (43.37 \pm 0.22)^\circ$ , and the phase of  $\eta_{+-}$ ,  $\phi_{+-} = (43.2 \pm 1.6)^\circ$ , which is predicted by CPT invariance to equal  $\phi_{SW}$ .

## INTRODUCTION

CP-violation was first discovered<sup>1)</sup> in 1964 in the  $\pi^+\pi^-$  decay of the long-lived neutral kaon ( $K_L$ ); this and subsequent measurements point to a very small asymmetry in the mixing of  $K^0$  and  $\bar{K}^0$ , which is parametrized by  $|\epsilon| \approx 2.3 \times 10^{-3}$ . Today it is thought that the Standard Model with three generations, so called six-quark model<sup>2)</sup> of Cabbibo, Kobayashi and Maskawa (CKM), can account for this phenomenon. In this model CP-violation arises from a non-zero phase in the  $V_{ub}$  transition matrix element through the now familiar "box diagram" shown in Fig.1.

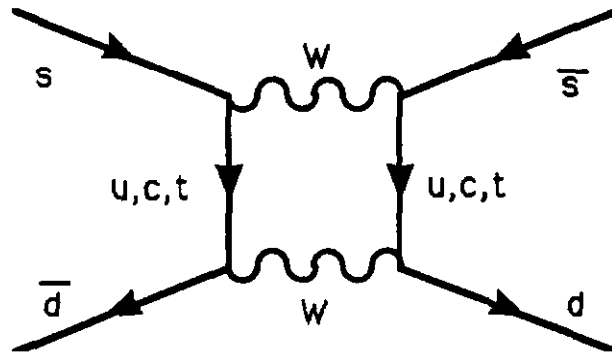


Figure 1: The  $\Delta S = 2$  "box diagram" in the Standard Model, which is a mixing between  $K^0$  and  $\bar{K}^0$ .

Until very recently, the only observed CP-nonconserving effect was consistent with asymmetric  $K^0$ - $\bar{K}^0$  mixing. This is a second-order effect (the box diagram) in the CKM framework, but could also signal a new  $\Delta S = 2$  interaction (e.g., Superweak<sup>3</sup>). The CKM mechanism has one consequence, a second manifestation of first-order  $\Delta S = 1$  ("direct") CP non-conservation in the  $K^0(\bar{K}^0) \rightarrow 2\pi$  decay itself is expected, parametrized by  $\epsilon'/\epsilon$ . That is to say, the CP-odd eigenstate in the  $K_L$  amplitude,  $K_2$ , will also decay to  $2\pi$ . This transition is described in part by the strong "penguin diagram" shown in Fig. 2, and by its electroweak counterparts, in which the gluon is replaced by a photon or a Z boson.<sup>4</sup>

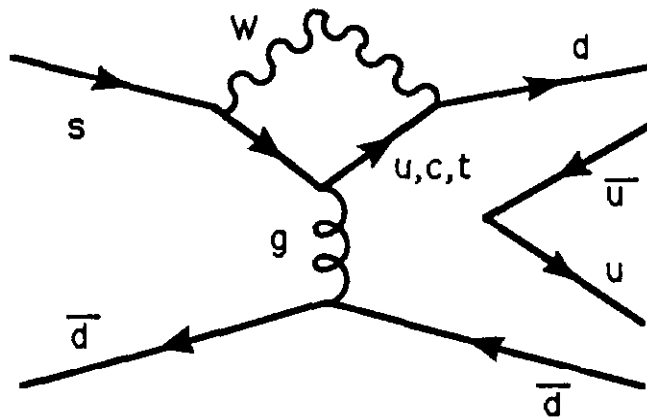


Figure 2: The strong "penguin diagram" contributing to  $K_2 \rightarrow \pi^+\pi^-$ , a "direct" CP violating term.

# LATEST RESULTS ON THE DIRECT CP VIOLATION MEASUREMENTS – $\epsilon'/\epsilon$

Yee B. Hsiung  
(E731 collaboration)  
*Fermi National Accelerator Laboratory, P. O. Box 500  
Batavia, Illinois 60510, U.S.A.*

## ABSTRACT

Preliminary results, based on the full data sample from Fermilab-E731 and the combined data sample from CERN-NA31, on the “direct” CP-violation measurements  $\epsilon'/\epsilon$  in neutral kaon decay have been reviewed. The E731’s result is  $Re(\epsilon'/\epsilon) = (6.0 \pm 5.8(\text{stat}) \pm 3.2(\text{syst}) \pm 1.8(\text{MC})) \times 10^{-4}$ , which provides no evidence for “direct” CP-violation, thus supporting the Superweak model; while the NA31’s combined result ('86+'88+'89 data) is  $Re(\epsilon'/\epsilon) = (23 \pm 3.4(\text{stat}) \pm 6.5(\text{syst})) \times 10^{-4}$ , three standard deviations from zero, which provides evidence for the “direct” CP-violation in the Standard Model. Comparisons of the two experiments are made. The Fermilab-E731 group has also fit for the other parameters of the neutral kaon system in their  $2\pi$  data sample, such as: the  $K_S$  life time  $\tau_S$ ; the  $K_L$ - $K_S$  mass difference  $\Delta m$ ; the phase difference between  $\eta_{00}$  and  $\eta_{+-}$ ,  $\Delta\phi = (-0.6 \pm 1.6)^\circ$ , Which is a test of CPT invariance; the Superweak phase  $\phi_{SW} = (43.37 \pm 0.22)^\circ$ , and the phase of  $\eta_{+-}$ ,  $\phi_{+-} = (43.2 \pm 1.6)^\circ$ , which is predicted by CPT invariance to equal  $\phi_{SW}$ .

## INTRODUCTION

CP-violation was first discovered<sup>1)</sup> in 1964 in the  $\pi^+\pi^-$  decay of the long-lived neutral kaon ( $K_L$ ); this and subsequent measurements point to a very small asymmetry in the mixing of  $K^0$  and  $\bar{K}^0$ , which is parameterized by  $|\epsilon| \approx 2.3 \times 10^{-3}$ . Today it is thought that the Standard Model with three generations, so called six-quark model<sup>2)</sup> of Cabbibo, Kobayashi and Maskawa (CKM), can account for this phenomenon. In this model CP-violation arises from a non-zero phase in the  $V_{ub}$  transition matrix element through the now familiar “box diagram” shown in Fig.1.

Search for such effect in the predicted range provide an important test of the Standard Model, while the Superweak model has no  $\Delta S = 1$  manifestation of the effect.

The  $K^0$  and  $\bar{K}^0$  are the strong interaction eigenstates in the production, because the strong interaction conserves strangeness. The kaon decays through the weak interaction allowed  $\Delta S = \pm 1$  transitions. They also mix with each other through intermediate  $S = 0$  states (e.g.  $2\pi$  and  $3\pi$ ). Taking into account the small CP violation,  $\varepsilon$ , in the  $K^0$ - $\bar{K}^0$  mixing, the vacuum eigenstates are:

$$K_{S,L} = [ (1+\varepsilon)K^0 \pm (1-\varepsilon)\bar{K}^0 ] / \sqrt{2(1+\varepsilon^2)},$$

where the plus sign is for  $K_S$  and the minus sign is for  $K_L$ . The parameter  $\varepsilon$  introduces a small CP-even impurity into the long-lived state ( $K_L$ ), allowing it to decay into the  $2\pi$  final states. The two complex parameters  $\eta_{+-}$  and  $\eta_{00}$  are defined as the ratios of  $K_L$  and  $K_S$  decay amplitudes into  $\pi^+\pi^-$  and  $\pi^0\pi^0$ , where

$$\eta \equiv \frac{\text{amp}(K_L \rightarrow \pi\pi)}{\text{amp}(K_S \rightarrow \pi\pi)}.$$

Neglecting a small ( $\approx 5\%$ ) violation of the  $\Delta I = \frac{1}{2}$  rule, we have:

$$\eta_{+-} \equiv |\eta_{+-}| e^{i\phi_{+-}} = \varepsilon + \varepsilon' \quad \text{and}$$

$$\eta_{00} \equiv |\eta_{00}| e^{i\phi_{00}} = \varepsilon - 2\varepsilon'.$$

Here,  $\varepsilon'$  parametrizes any additional CP-violation arising *directly* from the  $2\pi$  decay amplitudes, the “direct” CP-violation, and is written as

$$\varepsilon' = \frac{i}{\sqrt{2}} \frac{\text{Im}A_2}{\text{Re}A_0} e^{i(\delta_2 - \delta_1)},$$

where  $A_I$  is the decay amplitude of  $K^0$  into  $2\pi$  final state of isospin  $I$  with a phase shift  $\delta_I$  from the  $2\pi$  final state interactions, with an experimental value<sup>5)</sup>  $\delta_2 - \delta_0 = -45^\circ \pm 10^\circ$ . Experiments seek to isolate such an effect by measuring the double ratio  $R$  of the decay rates of  $K_L$  and  $K_S$  to  $\pi^+\pi^-$  and  $\pi^0\pi^0$ .

$$R = \frac{|\eta_{+-}|^2}{|\eta_{00}|^2} = \frac{\Gamma(K_L \rightarrow \pi^+ \pi^-)/\Gamma(K_S \rightarrow \pi^+ \pi^-)}{\Gamma(K_L \rightarrow \pi^0 \pi^0)/\Gamma(K_S \rightarrow \pi^0 \pi^0)} \equiv 1 + 6 \operatorname{Re}(\epsilon'/\epsilon).$$

Until about 15 years ago, the best available measurement put  $\operatorname{Re}(\epsilon'/\epsilon) < 0.02$ . Then, in 1977, the b quark was discovered, and it became possible to make Standard Model predictions for the value of  $\epsilon'$ . This in turn provided renewed motivation for new round of experiments, including Fermilab's E731 and CERN's NA31. The expected value of  $\operatorname{Re}(\epsilon'/\epsilon)$  is now below  $10^{-2}$ , this translates to a small deviation (less than a few percent) of  $R$  from unity. The controversy came from the previous published results<sup>6),7)</sup> between NA31's '86 data and E731 20% data sample, where

$$\operatorname{Re}(\epsilon'/\epsilon) = (33 \pm 11) \times 10^{-4} \quad \text{from NA31's '86 data,}$$

which supports an observation of "direct" CP-violation, and

$$\operatorname{Re}(\epsilon'/\epsilon) = (-4 \pm 15) \times 10^{-4} \quad \text{from E731's 20% data sample,}$$

which is definitely consistent with zero, thus *no* direct CP-violation! Recent theoretical calculation<sup>8)</sup> shows that, as the value of top quark mass increases, the expect value of  $\epsilon'/\epsilon$  decreases. This is due to the large cancelation between gluon-penguin and Z-penguin diagrams for  $m_t > 100$  GeV. Although one expects a significant non-zero value of  $\epsilon'$  in the Standard Model, the calculation is uncertain partly because  $m_t$  and  $V_{td}$  are not well known and primarily because of the difficulty of estimating hadronic matrix elements.<sup>9)</sup> The theoretical results for  $\epsilon'/\epsilon$  in the Standard Model are generaally in the range  $3 \times 10^{-4}$  to  $5 \times 10^{-3}$ . Since then, new data have been taken by NA31 collaboration, and the remaining E731 data have also been analyzed to improve the precision of  $\epsilon'/\epsilon$  to better than  $10^{-3}$ .

## CHALLENGES AND DIFFICULTIES

As discussed earlier, to extract  $\epsilon'/\epsilon$ , one needs accurate counting the decay rates for  $K_L$  and  $K_S$  into both  $\pi^+\pi^-$  and  $\pi^0\pi^0$ . Because of the

smallness of  $Re(\epsilon'/\epsilon)$ , it is important to minimize the systematic uncertainty in the collection and analysis of the four decay modes. To achieve the accuracy below  $10^{-3}$  on  $\epsilon'/\epsilon$ , one needs to keep the following systematics between  $K_L$  and  $K_S$  decaying into  $\pi^+\pi^-$  or  $\pi^0\pi^0$  understood to better than  $10^{-3}$ , such as backgrounds, acceptance corrections, detector asymmetries, efficiencies and gain drifts, as well as accidental rate effects. In another word, for accurate counting, one needs to worry about event losses or gains, either at the data collection time and analysis stage or at the Monte Carlo corrections to the acceptance and to the accidental rate effects. Therefore the understanding of the detector performance, the simulation of the detector resolution and detector bias are quite important, especially for the electromagnetic calorimeter which is used in the  $2\pi^0$  mode.

The branching ratio for  $K_L$  to  $2\pi^0$  (or  $\pi^+\pi^-$ ) decay is small, only 0.1% (0.2%), therefore one needs to reduce the large background from  $3\pi^0$  (or  $\pi^+\pi^-\pi^0$ ,  $\pi e\nu$  and  $\pi\mu\nu$ ) decays. This requires not only a good detection efficiency and good resolution for  $\gamma$  (as well as for charged pion), but also a good veto efficiency on wide angle escaping  $\gamma$  (as well as rejection on electrons and muons). Nearly hermetic annular  $\gamma$  veto coverage surrounding the decay region and two beam holes is necessary to reduce the  $3\pi^0$  background to less than a percent level. The geometrical acceptance of the detector should be as simple as possible to avoid complicated apertures, edges and holes for the acceptance corrections between these four modes. Since the vertex of the  $2\pi^0$  decay depends only on the measured energy and position of photons from the electromagnetic calorimeter, the relative energy scale, which determines the distance scale of the longitudinal decay vertex between  $2\pi^0$  and  $\pi^+\pi^-$ , must be understood quite well to about  $10^{-3}$  level.

## THE CERN NA31 EXPERIMENT

The NA31 experiment (CERN, Edinburgh, Mainz, Orsay, Pisa, Siegen) shown in Fig. 3, chose to count  $\pi^0\pi^0$  and  $\pi^+\pi^-$  decays at the same time by using *purely* calorimetric detectors for the reconstruction of the

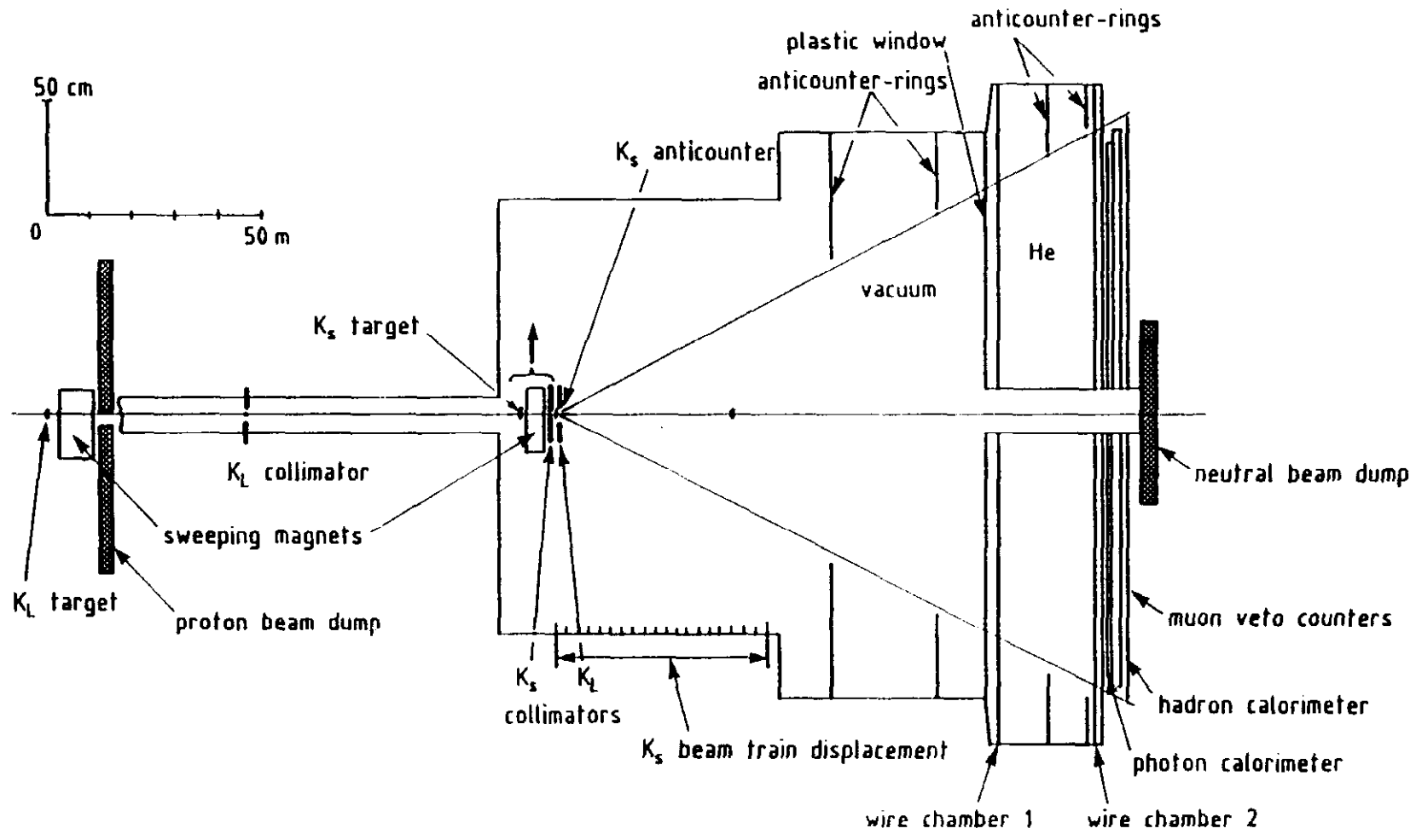


Figure 3: NA31 experiment layout.

particle energies, and then alternating data taking between  $K_L$  and  $K_S$  mini-periods. The double ratio  $R$  was then taken as

$$R = \frac{R_L}{R_S} = \frac{\Gamma(K_L \rightarrow \pi^0 \pi^0)/\Gamma(K_L \rightarrow \pi^+ \pi^-)}{\Gamma(K_S \rightarrow \pi^0 \pi^0)/\Gamma(K_S \rightarrow \pi^+ \pi^-)} = \frac{N_L^{00}/N_L^{+-}}{N_S^{00}/N_S^{+-}}.$$

The  $\pi^0\pi^0 \rightarrow 4\gamma$  decays (neutral mode) were collected by the liquid argon calorimeter (LAC), while the  $\pi^+\pi^-$  decays (charged mode) were measured by wire chambers in front of the LAC for the vertex determination and a hadron calorimeter for the energy measurement. No magnet was used in this experiment to keep the geometric acceptance simple. A 50 m long vacuum decay region was used to collect  $K_L$  and  $K_S$  decays. There were two target stations, the upstream target used for the  $K_L$  run and the downstream target train (with 41 stations) used for the  $K_S$  run. The  $K_S$  target train was moving throughout the decay region (with 1.2m steps) thereby minimizing the acceptance corrections for  $K_S$  vs  $K_L$  decays due to very different lifetimes. Figure 4 shows the similar  $\pi^+\pi^-$  decay vertex  $z$  distributions for  $K_L$  and  $K_S$  over a 50m decay region after proper weighting over the  $K_S$  target stations. During the  $K_L$  runs, 450 GeV protons were extracted to strike the far target with an intensity of  $10^{11}$  protons per pulse. For the  $K_S$  runs, 360 GeV protons were used to strike the  $K_S$  target train with an intensity of  $10^7$  protons per pulse. Thus the accidental effects due to different beam intensities (rate effects) have to be corrected for all four decay modes.

Since the experiment has to normalize  $\pi^0\pi^0$  decays to  $\pi^+\pi^-$  decays in each  $K_L$  and  $K_S$  mini-period, a good monitor on gain drifts, trigger and veto efficiencies as well as chamber efficiencies *verses* time is very important. The collaboration took data in '86, '87, '88 and '89, in which the '87 run was dedicated to the CPT measurement of  $\phi_{+-}$  and  $\phi_{00}$  phase difference. The preliminary results<sup>10)</sup> based on the combined data from '86, '88 and '89 runs, announced at '91 Lepton-Photon conference in Geneva, are summarized here.

The  $\pi^+\pi^-$  decays were selected by the following criteria: (1)  $\geq 2$  hits in each wire chamber, hits in charged hodoscope and no veto counter

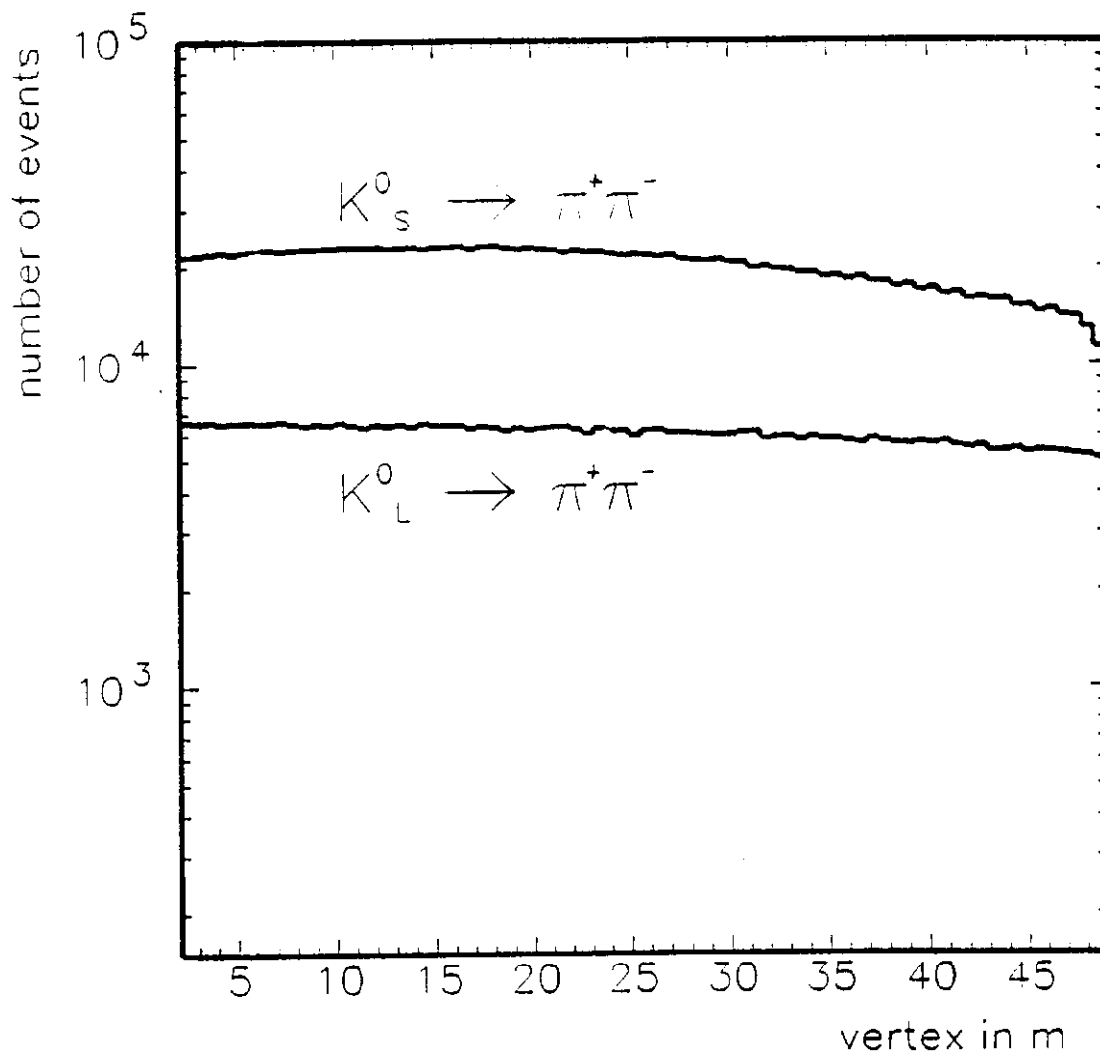


Figure 4: NA31  $K_{S,L} \rightarrow \pi^+ \pi^-$  decay z-vertex distributions after proper weighting the  $K_S$  target stations.

signals, (2) longitudinal energy ratio cut of each track in calorimeter to reject  $K_{e3}$ , (3) energy ratio cut of tracks,  $0.4 < E_1/E_2 < 2.5$ , to reject  $\Lambda \rightarrow p\pi^-$  background, (4) no additional photons in LAC (removes  $K_{\pi3}$ ), (5) track separation and distance away from beam axis, (6) total calorimeter energy  $> 40$  GeV. Typically 30% events were lost due to the  $p/\pi$  energy ratio cut from the hadron calorimeter to suppress the  $\Lambda$  backgrounds. The decay vertex of  $\pi^+\pi^-$  was determined by using hits in the wire chambers, which had a  $500\mu\text{m}$  resolution per plane. The kaon energy,  $E_K$ , was reconstructed kinematically by using the ratio of track energies from the calorimeter and the track opening angle  $\Theta$ , as

$$E_K = \frac{1}{\Theta} \sqrt{T} \sqrt{m_K^2 - m_\pi^2 T}$$

where

$$T = 2 + \frac{E_1}{E_2} + \frac{E_2}{E_1}.$$

A typical  $\pi^+\pi^-$  mass distribution for  $K_L$  and  $K_S$  is shown in Fig. 5, in which the  $\pi^+\pi^-\pi^0$  backgrounds are peaked below 0.4 GeV for the  $K_L$  decay. Figure 6 shows the distribution of reconstructed transverse distance of kaon to the target (D-target) for the overlays of  $K_L$  and  $K_S$  to  $\pi^+\pi^-$  decays, where the signal region is defined as D-target  $< 5\text{cm}$ . The backgrounds from  $K_{e3}$ ,  $K_{\mu3}$  and  $K_{\pi3}$  were simulated for  $K_L$  as shown in Fig. 7. The individual background fractions are summarized in Table 1. The total  $\pi^+\pi^-$  background was estimated to be  $0.9\% \pm 0.15\%$  for  $K_L$ , and  $0.06\%$  for  $K_S$  in their '88 data.

The  $\pi^0\pi^0 \rightarrow 4\gamma$  decays were reconstructed from the measured positions and energies of the photons. The distance of the decay  $z$  vertex from the calorimeter was calculated, using  $K^0$  mass as a constraint, as

$$z = \frac{1}{m_K} \sqrt{\sum_{\gamma \text{ pairs}} E_i E_j d_{ij}^2}.$$

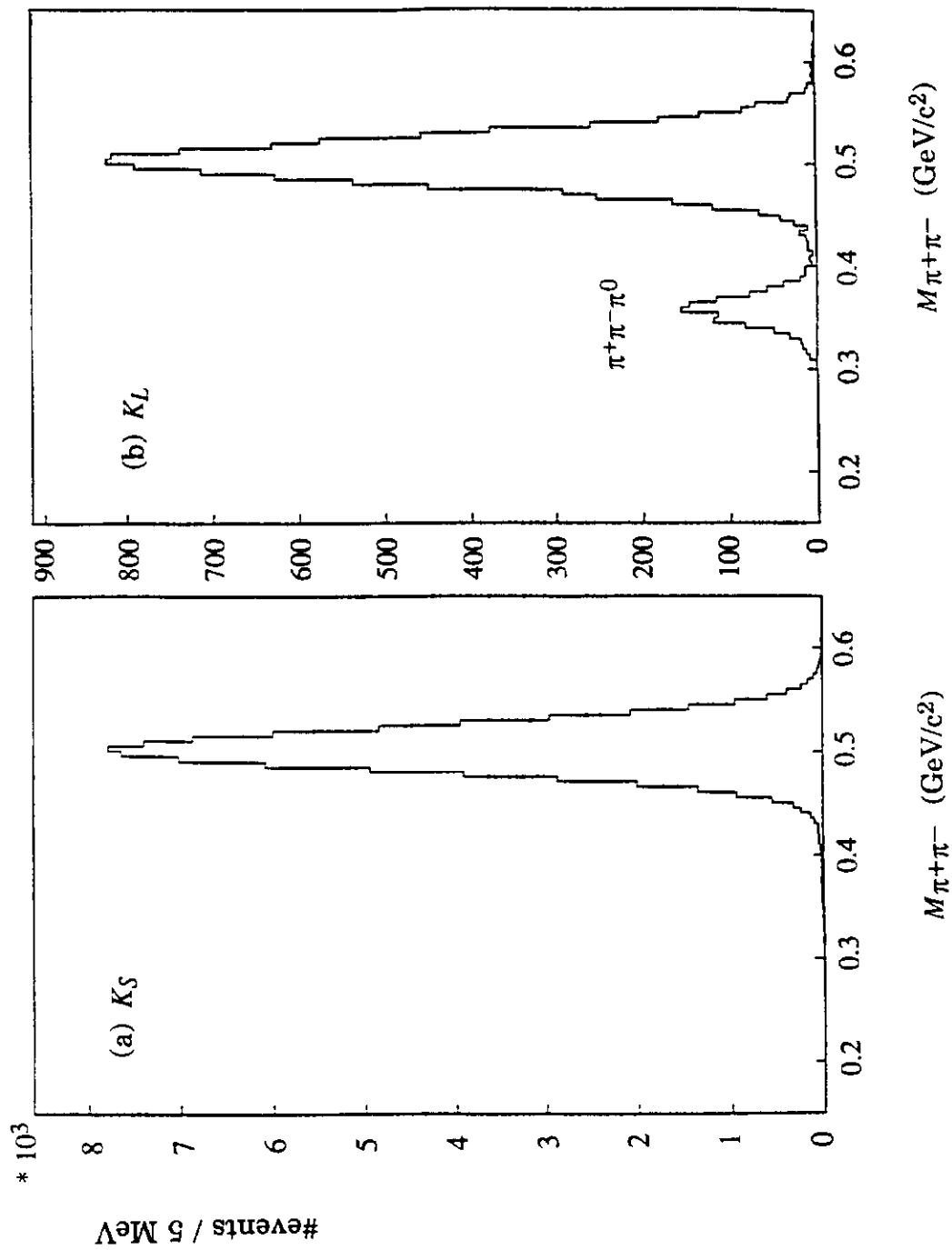


Figure 5: Typical NA31  $\pi^+\pi^-$  mass distributions for (a)  $K_S$  and (b)  $K_L$ . The mass resolution is between 20 to 28 MeV.

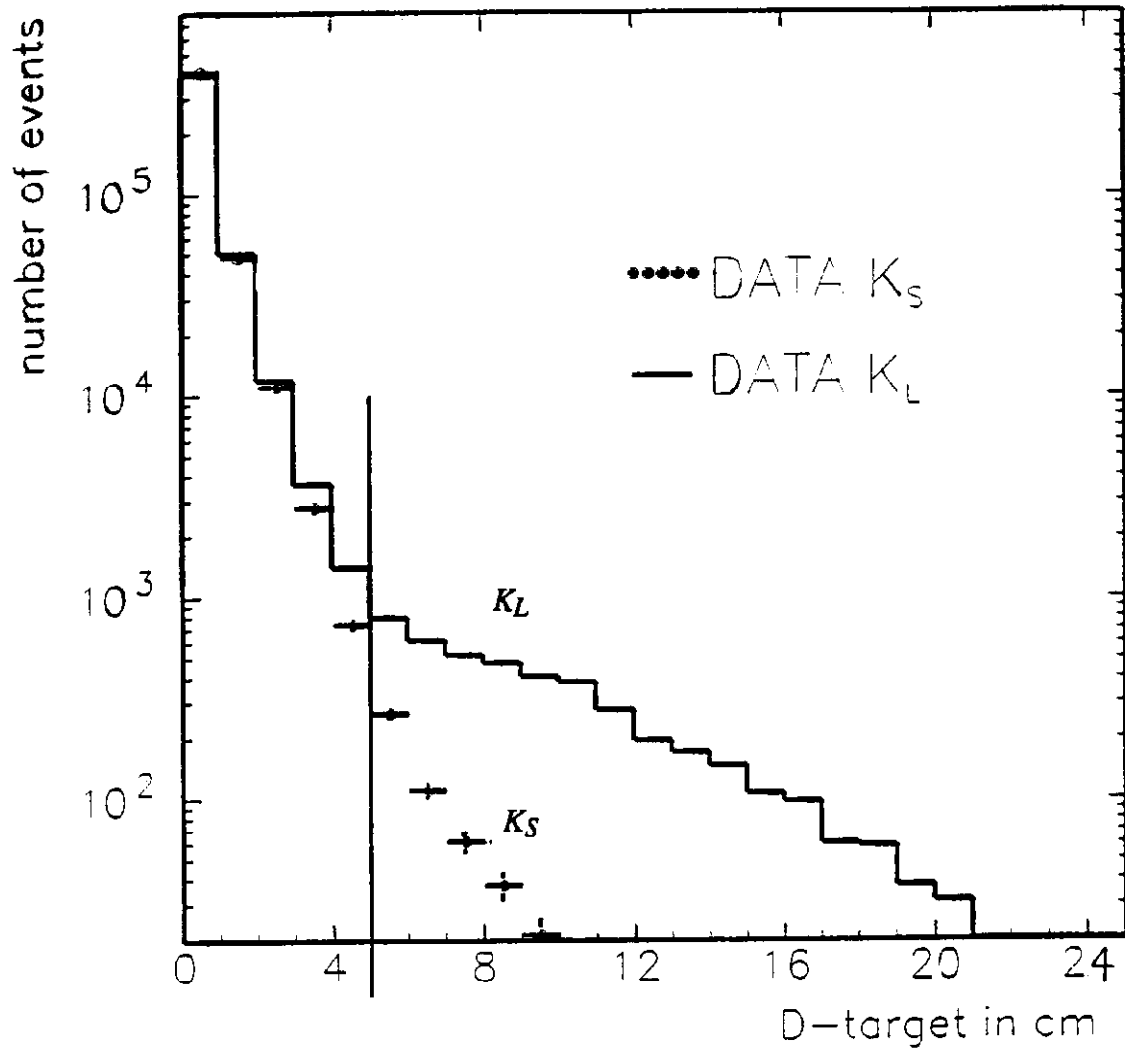


Figure 6: D-target distribution for  $K_{S,L} \rightarrow \pi^+\pi^-$  in NA31. The reconstructed transverse distance to target with a 5cm cut.

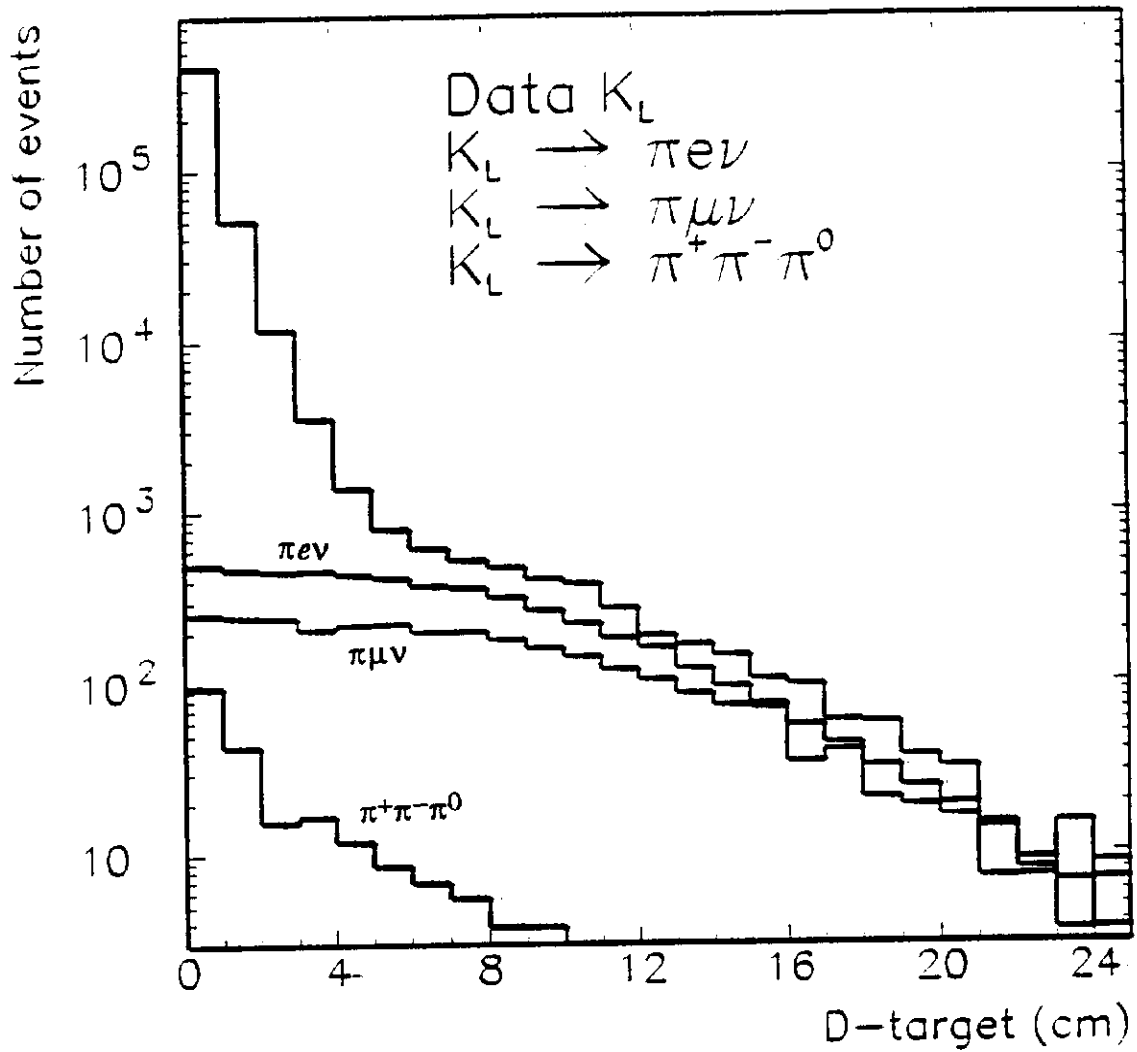


Figure 7: NA31's background simulation in  $K_L \rightarrow \pi^+ \pi^-$ , three background contributions,  $\pi e \nu$ ,  $\pi \mu \nu$  and  $\pi^+ \pi^- \pi^0$ .

Table 1: Summary of NA31's backgrounds for '88 data

| Mode                         | Background process                | Background level | Background subtotal |
|------------------------------|-----------------------------------|------------------|---------------------|
| $K_L \rightarrow \pi^+\pi^-$ | $K_{e3}$                          | 0.49%            | $0.9\% \pm 0.15\%$  |
|                              | $K_{\mu 3}$                       | 0.25%            |                     |
|                              | $K_{\pi 3}$                       | 0.04%            |                     |
|                              | $n \rightarrow \pi^+\pi^-X$       | 0.12%            |                     |
| $K_S \rightarrow \pi^+\pi^-$ | $\Lambda \rightarrow p\pi^-$      | 0.01%            | 0.06%               |
|                              | $n \rightarrow \pi^+\pi^-X$       | 0.06%            |                     |
| $K_L \rightarrow \pi^0\pi^0$ | $K_L \rightarrow \pi^0\pi^0\pi^0$ | 2.6%             | $2.6\% \pm 0.17\%$  |
| $K_S \rightarrow \pi^0\pi^0$ |                                   | none             |                     |

Both  $K^0$  energy and decay  $z$  vertex were measured to about 1% in accuracy. The event selections were (1) no hits in wire chambers, hits in neutral hodoscope from conversion and no hits in veto counters, (2) four reconstructed photons in LAC ( $> 5\text{cm}$  separation), (3) photon energy cut,  $3 \text{ GeV} < E_\gamma < 100 \text{ GeV}$ , (4) center of gravity  $< 10\text{cm}$  from the beam axis, (5) kaon energy between 60 to 180 GeV, (6) decay  $z$  vertex cut. Constraints on the masses of two photon pairs were used to reduce the background from  $K_L \rightarrow 3\pi^0$ , mainly due to escaping photons because of not enough  $\gamma$  veto coverage. This background was distributed in a scatter plot of photon-pair masses, as seen in Fig. 8. Signal and background events were counted in equal-area  $\chi^2$  contours around the  $\pi^0$  mass region defined for the accepted events. The signal region was taken as  $\chi^2 < 9$  as shown in Fig. 9. The  $3\pi^0$  background in  $K_L \rightarrow 2\pi^0$  was estimated to be  $2.6\% \pm 0.17\%$ . This is done by overlaying the  $3\pi^0$  background simulation over the data and extrapolated into the signal region as seen in Fig. 9. The background in  $K_S \rightarrow 2\pi^0$  was negligible. The statistics from '88 and '89 runs are summarized in Table 2. Nearly a factor of 2 improvements in statistics for the '89 run. About 400k  $K_L \rightarrow \pi^0\pi^0$  events were collected in total when all the data from '86, '88 and '89 are combined together.

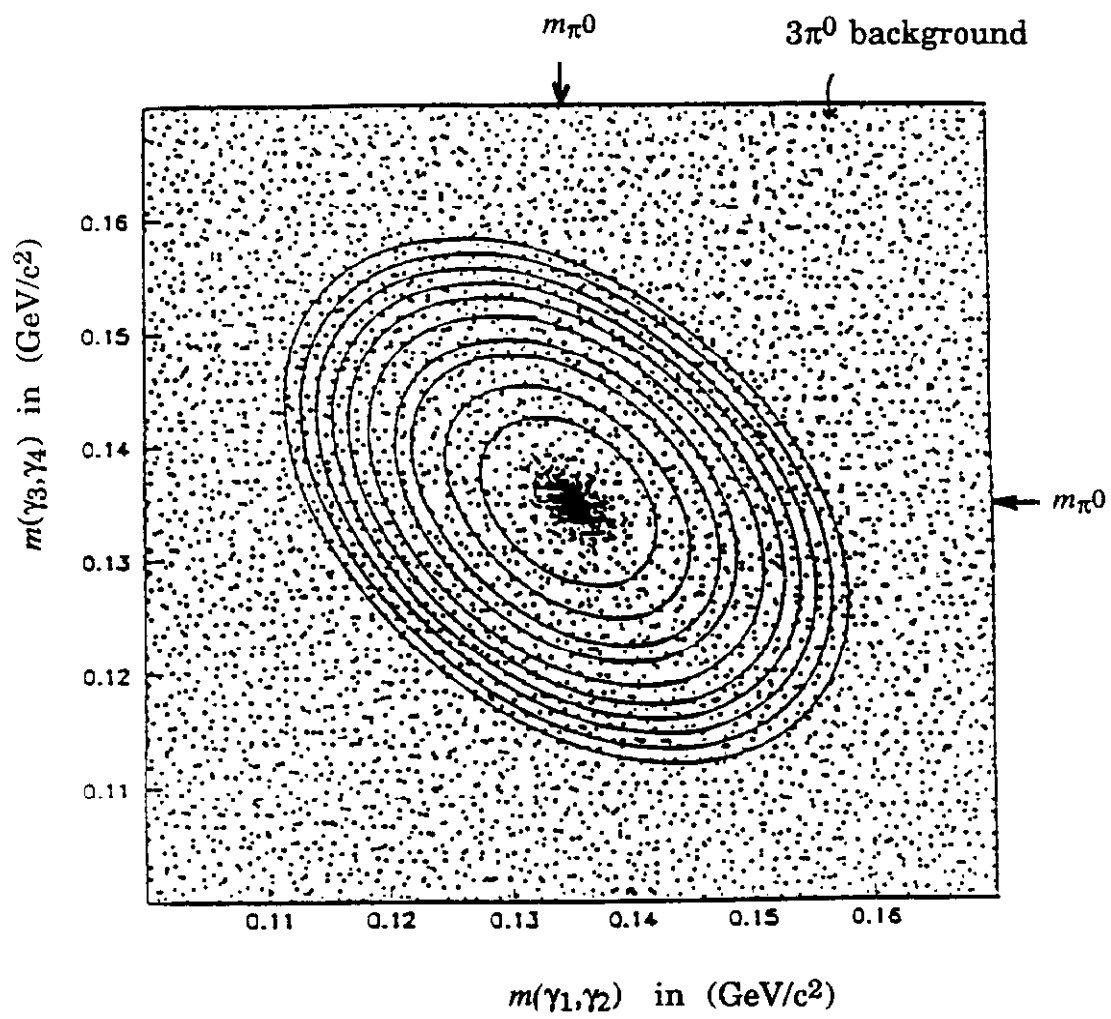


Figure 8: Scatter plot of photon pair masses, *i.e.*  $m(\gamma_1, \gamma_2)$  versus  $m(\gamma_3, \gamma_4)$ , for  $K_L \rightarrow \pi^0 \pi^0$ . The elliptical contours are the equal-area  $\chi^2$  contours around the  $\pi^0$  mass region for  $3\pi^0$  background determination.

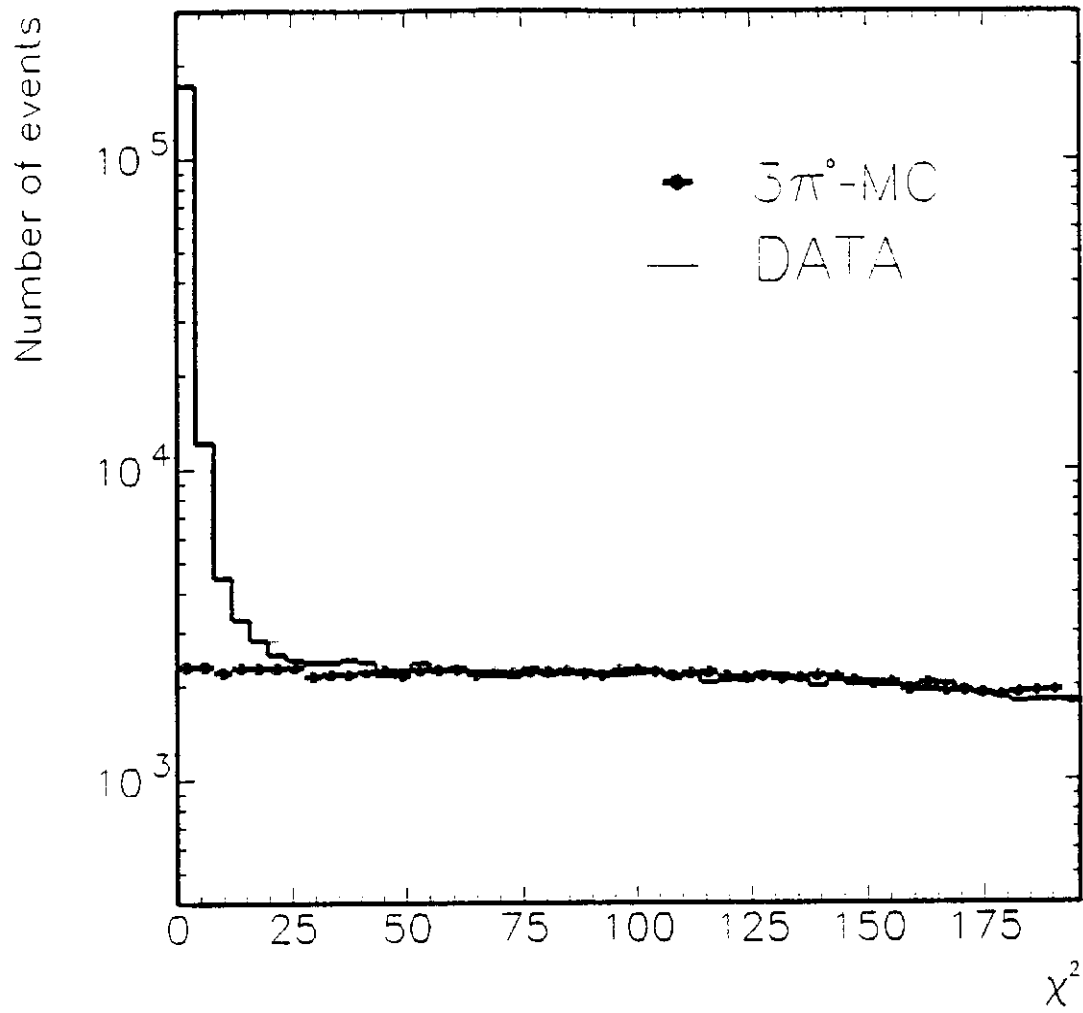


Figure 9: NA31  $3\pi^0$  background simulation for  $K_L \rightarrow \pi^0\pi^0$  in equal-area  $\chi^2$  plot. The signal region is defined as  $\chi^2 < 9$ .

Table 2: NA31's statistics from '88 and '89 data.

| Mode                         | '88 data | '89 data<br>Preliminary |
|------------------------------|----------|-------------------------|
| $K_L \rightarrow \pi^0\pi^0$ | 110k     | 180k                    |
| $K_L \rightarrow \pi^+\pi^-$ | 290k     | 470k                    |
| $K_S \rightarrow \pi^0\pi^0$ | 560k     | 630k                    |
| $K_S \rightarrow \pi^+\pi^-$ | 1380k    | 1530k                   |

### THE NA31 RESULTS

To extract  $\epsilon'/\epsilon$ , the analysis divided the data into mini-periods, 12 energy bins and 39 decay  $z$  vertex bins, and calculated the double ratio  $R$  in each bin, then averaging over bins. The raw double ratios are shown in Table 3 with necessary corrections from accidental effect and other differences between  $K_L$  and  $K_S$ . Accidental corrections due to rate effect which causes event loss or gain, were made by studying the effect of overlaying random events (taken during the runs) with good real events in each mode, then pass through the reconstruction. The corrections to the double ratio  $R$  were  $+0.05\% \pm 0.12\%$  (stat.)  $\pm 0.2\%$ (syst.) for '88 data and  $-0.48\% \pm 0.08\%$  (stat.)  $\pm 0.2\%$ (syst.) for '89 data (note: 0.6% changes in  $R$  corresponds to  $10^{-3}$  changes in  $\epsilon'/\epsilon$ ). Corrections due to different  $K_L$  and  $K_S$  beam divergence, different energy spectra, resolution smearing and binning, scattering of events in  $K_S$  and anti-counter inefficiencies, were also simulated in a monte carlo with a total MC corrections of  $+0.23\% \pm 0.09\%$ (stat.). The main contributions were  $+0.5\%$  due to beam divergence and  $-0.4\%$  due to scattering in  $K_S$ . Other corrections were  $+0.41\%$  for '88 data and  $+0.56\%$  for '89 data (presumably due to the corrections on efficiencies, but it was not clear to the author).

The systematic errors for '88 data are listed in Table 4, which give  $\pm 0.4\%$  total systematic error in double ratio  $R$ . Same systematic errors are assumed for the preliminary result of '89 data. This corresponds to a systematic error of  $\pm 7 \times 10^{-4}$  on  $\epsilon'/\epsilon$ .

Table 3: Corrections on double ratio  $R$  for '88 and '89 data.

| Double Ratio             | '88 data<br>final result        | '89 data<br>preliminary         |
|--------------------------|---------------------------------|---------------------------------|
| $R_{\text{raw ratio}}$   | $0.983 \pm 0.004$               | $0.985 \pm 0.003$               |
| Accidental Corr.         | +0.0005                         | -0.0048                         |
| Monte Carlo Corr.        | +0.0023                         | +0.0022                         |
| Other Corrections        | +0.0041                         | +0.0056                         |
| $R$                      | $0.990 \pm 0.004(\text{stat.})$ | $0.988 \pm 0.003(\text{stat.})$ |
| $Re(\epsilon'/\epsilon)$ | $(17 \pm 7) \times 10^{-4}$     | $(21 \pm 5) \times 10^{-4}$     |

Table 4: Systematic errors of NA31's '88 data

| Systematics               | Errors on double ratio $R$ |
|---------------------------|----------------------------|
| $\pi^+\pi^-$ background   | $\pm 0.15\%$               |
| $\pi^0\pi^0$ background   | $\pm 0.17\%$               |
| Energy calib. & stability | $\pm 0.14\%$               |
| Inefficiencies            | $\pm 0.23\%$               |
| Monte Carlo statistics    | $\pm 0.1\%$                |
| Accidental overlay        | $\pm 0.2\%$                |
| Total                     | $\pm 0.4\%$                |

Therefore combining the statistical and systematic errors, the NA31 results on  $\epsilon'/\epsilon$  are

$$Re(\epsilon'/\epsilon) = (17 \pm 10) \times 10^{-4} \quad \text{for '88 data,}$$

$$Re(\epsilon'/\epsilon) = (21 \pm 9) \times 10^{-4} \quad \text{for '89 data (preliminary).}$$

Combining with their previous published result,<sup>6)</sup>

$$Re(\epsilon'/\epsilon) = (33 \pm 11) \times 10^{-4} \quad \text{from '86 data,}$$

and taking into account the correlated errors, gives the final combined result,

$$Re(\epsilon'/\epsilon) = (23 \pm 7) \times 10^{-4} \quad \text{for '86 + '88 + '89 data,}$$

in which the total statistical error is  $\pm 3.4 \times 10^{-4}$  and the total systematic error is  $\pm 6.5 \times 10^{-4}$ . Even though, both '88 and '89 results are about one standard deviation lower than the '86 result, the final combined result (including '86 data) is still three standard deviations from zero. This result, although dominated by the systematic error, supports the direct CP-violation in the Standard Model and excludes the Superweak model (at 99% C.L.). Clearly the systematic uncertainty ( $6.5 \times 10^{-4}$ ) is now dominating the NA31's total error on  $\epsilon'/\epsilon$  when combined all their data together and it is hard to reduce it further.

### THE FERMILAB EXPERIMENT E731

The E731 experiment (Chicago, Elmhurst, Fermilab, Princeton and Saclay) shown in Fig. 10, chose to collect  $K_L$  and  $K_S$  decays *simultaneously* with the *same* detector for either  $\pi^0\pi^0$  or  $\pi^+\pi^-$  mode. A double  $K^0$  beam technique was used to minimize the possible systematic uncertainties. This was done by producing two nearly identical and parallel  $K_L$  beams and then obtaining  $K_S$  by placing a regenerator in one beam. The coherently regenerated  $K_S$  ensured an angular divergence identical to that of  $K_L$  and a very similar momentum spectrum. The double ratio  $R$  was then taken as

$$R = \frac{R_{00}}{R_{+-}} = \frac{|\eta_{00}|^2}{|\eta_{+-}|^2} = \frac{\Gamma(K_L \rightarrow \pi^0 \pi^0)/\Gamma(K_S \rightarrow \pi^0 \pi^0)}{\Gamma(K_L \rightarrow \pi^+ \pi^-)/\Gamma(K_S \rightarrow \pi^+ \pi^-)} = \frac{N_L^{00}/N_S^{00}}{N_L^{+-}/N_S^{+-}}.$$

Such an approach provided an automatic normalization (measuring  $|\eta_{00}|^2$  and  $|\eta_{+-}|^2$  directly) while making the measurements insensitive to variations in detection and analysis efficiencies which may arise from changes in gains, thresholds, dead times, counting rates, etc. during the data taking. Frequently moving the regenerator between two beams cancels the biases from beam or detector asymmetries. Since  $K_L$  and  $K_S$

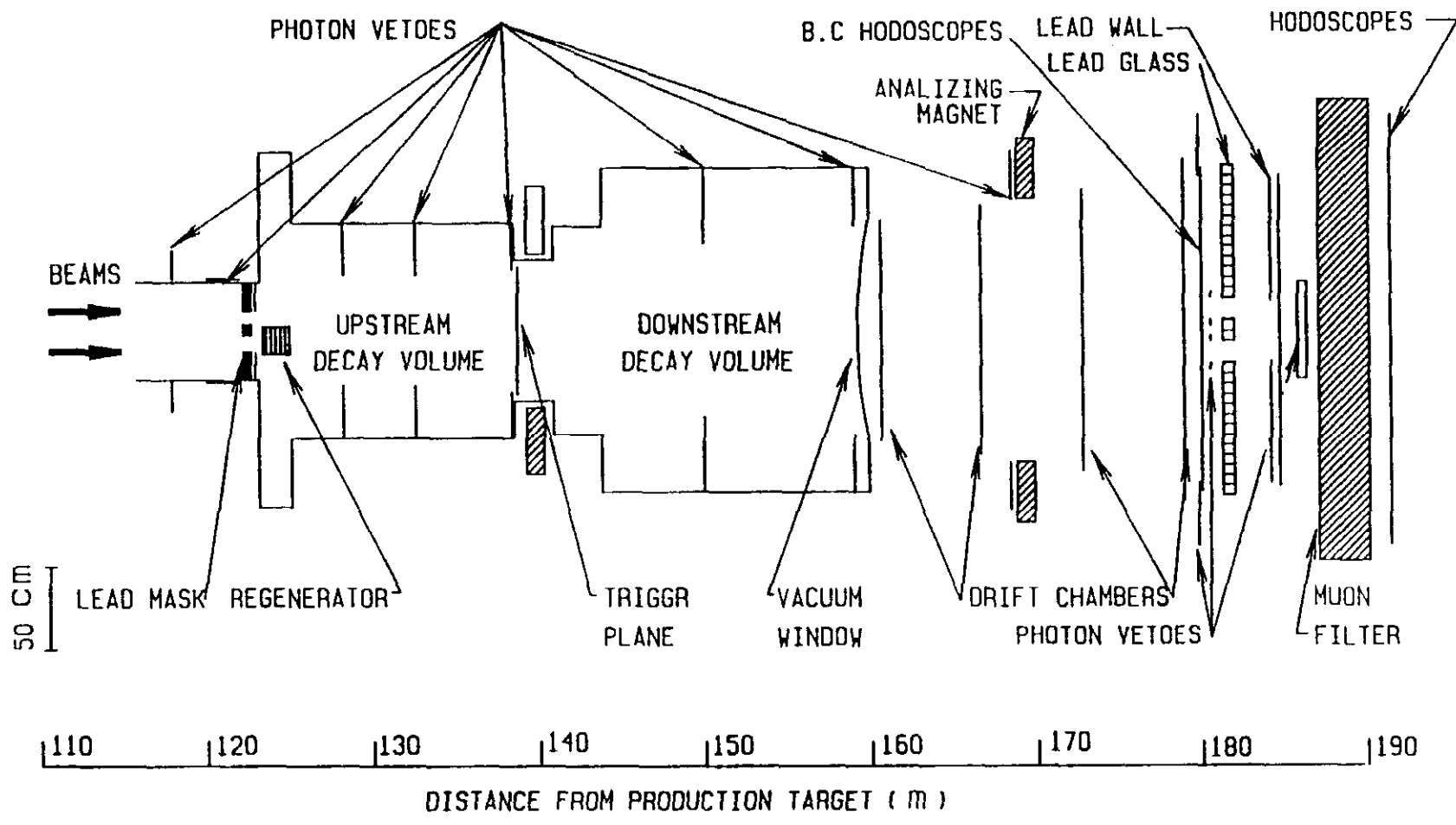


Figure 10: E731 experiment layout elevation view.

decays were collected at the same time, the exactly same selection criteria and kinematic cuts could be applied in either charged or neutral events to ensure correct event counting. A event was distinguished as a  $K_L$  or  $K_S$  decay (by the beam in which they decay) only after the event passed all analysis cuts.

The  $\pi^0\pi^0 \rightarrow 4\gamma$  decays (neutral mode) were collected by the lead-glass calorimeter, while the  $\pi^+\pi^-$  decays (charged mode) were measured by magnetic spectrometer consists of four drift chambers and an analyzing magnet for the determination of track momentum and decay vertex. The lead-glass calorimeter consisted of a circular array of 804 blocks of lead-glass bars (a fly's eye geometry). Each block is  $5.8\text{cm} \times 5.8\text{cm}$  in size transversely and 19 radiation-lengths( $X_0$ ) long. Photons from  $\pi^0\pi^0$  decays were measured with an energy resolution of  $2.5\% + 5\%/\sqrt{E}$  ( $E$  in GeV) and a linearity of better than  $\pm 0.1\%$  (after exacting calibration).

The  $K^0$  were produced by 800 GeV protons incident at 5 mrad on a beryllium target, after which collimators and sweeping magnets produced two side-by-side neutral kaon beams. The two beams were separated by 23 cm at the calorimeter. The average kaon energy was about 70 GeV.

The  $K_S$  was provided by coherent regeneration in a two interaction-lengths boron-carbide ( $B_4C$ ) regenerator placed about 123m downstream of target. The regenerator was instrumented with veto counters to reject inelastic regeneration. The regeneration of  $K_S$  comes about because of the cross sections difference between the  $K^0$  and  $\bar{K}^0$  in the matter. An incident  $K_L$ , that is one particular linear combination of  $K^0$  and  $\bar{K}^0$ , will turn into a different linear combination, thus picking up a  $K_S$  component. Only the coherently scattered kaons (in the forward direction) have the same beam profile and angular divergence as the original  $K_L$  beam. By instrumenting the regenerator with scintillators and phototubes, we rejected a good fraction of the inelastically scattered kaons at trigger level. The remaining small incoherently scattered

kaons (diffractive and inelastic) were subtracted using the kaon transverse momentum ( $p_t^2$ ) or some other similar variable.

A 14 m decay region downstream of the regenerator was used to collect both  $K_L$  and  $K_S$  decays simultaneously. The end of decay region was defined by a pair of thin scintillator planes (see Fig. 10), which were used in trigger for charged mode and in veto for neutral mode. A thin lead sheet converter ( $0.1 X_0$ ) was rolled in between the pair of scintillator planes for most of neutral mode running ( $\sim 70\%$ ). Event triggers were designed to be simple and unbiased. For charged decays, hodoscope and chamber signals were used to require a topology consistent with a non-muon two-body decay. The  $K_{\mu 3}$  ( $\pi\mu\nu$ ) decay was rejected with a muon hodoscope behind 3m of iron, the muon filter. This yielded large  $K_{e3}$  ( $\pi e\nu$ ) and  $\pi^+\pi^-\pi^0$  calibration samples. For neutral mode, the trigger requires four isolated electromagnetic clusters (with each cluster's energy greater than 1 GeV) and a total energy of about 28 GeV. Prescaled six-cluster triggers were also recorded to obtain a large  $\pi^0\pi^0\pi^0$  sample to fix detector parameters. The main background of  $\pi^0\pi^0$  comes from  $3\pi^0$  decays where two photons escape the lead-glass or emerge with other photons. To suppress this background, eleven planes of photon veto counters (nearly hermetic) were employed to intercept photons missing the lead-glass. The calorimeter was followed by a hadron veto consisting of a lead wall and a scintillator hodoscope.

At downstream of regenerator, as a function of proper time  $t$  from the regenerator, the  $\pi\pi$  decay rates in the vacuum ( $K_L$ ) beam and regenerated ( $K_S$ ) beam are proportional to  $|\eta|^2$  and  $|\rho \exp(-t/2\tau_S + i\Delta m t) + \eta|^2$ , respectively; where  $\rho$  is the coherent regeneration amplitude,  $\tau_S$  is the  $K_S$  lifetime,  $\Delta m$  is the  $K_L$ - $K_S$  mass difference, and  $\eta$  is the appropriate ratio of  $K_L$ -to- $K_S$  decay amplitudes. Because  $|\rho| \gg |\eta|$ , the ratio of the total number of regenerated to vacuum charged (neutral) decays  $R_{\pm}$  ( $R_{00}$ ) is proportional to  $|\rho/\eta_{\pm(00)}|^2$ . Thus,  $R \approx R_{\pm}/R_{00}$ .

The data taking took place between July 1987 and February 1988, which most of the data had charged mode and neutral mode taken *separately*, as seen in Table 5. Each data set had its own calibration and

alignment constants. The last 25% data sample (G and H sets) where *all four modes* were taken *simultaneously*, provided a very good check of systematics. The previous published result,<sup>7)</sup>  $Re(\epsilon'/\epsilon) = (-4 \pm 14(\text{stat.}) \pm 6(\text{syst.})) \times 10^{-4}$ , based only on the 20% data sample (G set), is clearly consistent with  $\epsilon'/\epsilon = 0$ . Since then, the remaining 80% data have been analyzed with much better understanding of the detector acceptance, detector response, as well as the background subtractions. The preliminary results<sup>11)</sup> from the full E731 data set, announced at '91 Lepton-Photon conference in Geneva, are summarized below.

Table 5: E731 data collection for 138 days' running.

| Data Set | # Running Days | Running Mode | Intensity [10 <sup>11</sup> ppp] | Pb Conversion Sheet |
|----------|----------------|--------------|----------------------------------|---------------------|
| A        | 5              | charged      | 3                                | no                  |
| B        | 25             | neutral      | 20                               | yes                 |
| B/C      | 10             | charged      | 3                                | no                  |
| C        | 16             | neutral      | 20                               | yes                 |
| D        | 18             | charged      | 3                                | no                  |
| E1       | 15             | neutral      | 20                               | yes                 |
| E2       | 10             | neutral      | 20                               | no                  |
| F        | 10             | charged      | 3                                | no                  |
| G        | 23             | both         | 8                                | no                  |
| H        | 6              | both         | 8                                | no                  |

### E731 ANALYSIS

The  $\pi^+\pi^-$  events were selected by the following criteria: (1) two opposite-charged tracks reconstructed by the 16 planes drift chamber system, (2) each track momentum  $p > 7$  GeV/c, (3) reject  $\Lambda \rightarrow p\pi^-$  by using track momenta ratio  $p_1/p_2 > 3$  and  $E_{p\pi} > 100$  GeV and  $|m_{p\pi} - m_\Lambda| < 10$  MeV/c<sup>2</sup>, (4) reject  $K_{e3}$  by cutting  $E/p < 0.80$ , where  $E$  is the energy in the lead glass calorimeter and  $p$  is the track momentum, (5) aperture cuts in the spectrometer. The event loss due to cuts were small, in which the

biggest loss is  $E/p$  cut amounts to 4%. The  $\pi^+\pi^-$  invariant mass was calculated assuming the charged pion mass for each track. Projecting the reconstructed kaon back from the decay vertex to the regenerator plane, the transverse momentum ( $p_t$ ) was determined with respect to a line from the target. Figure 11 shows the  $\pi^+\pi^-$  invariant mass of  $K_L$  and  $K_S$  after  $p_t^2 < 250$  (MeV/c)<sup>2</sup> cut. The kaon mass resolution is about 3.5 MeV/c<sup>2</sup>, and the line shape is identical between  $K_L$  and  $K_S$  decays. The signal region is defined to be 484 to 512 MeV/c<sup>2</sup>. The radiative  $\pi^+\pi^- \gamma$  low-side tail in  $K_S$  is clearly seen. The square of the transversed momentum ( $p_t^2$ ) is plotted in Fig. 12 for kaons with good mass in  $K_S$  (the regenerated beam), where the incoherent background is fitted to a functional form with exponential terms representing the diffractive and inelastic contributions. With a cut of 250 (MeV/c)<sup>2</sup>, the background under the coherent peak is found to be  $(0.150 \pm 0.011)\%$ . The corresponding background in  $K_L$  (the vacuum beam), as shown in Fig. 13, is  $(0.339 \pm 0.015)\%$ , which is mainly due to the residual  $\pi e \nu$  decays.

The decay vertex for  $K_{L,S} \rightarrow \pi^0\pi^0$  decays was found by pairing the photons using the known  $\pi^0$  mass as a constraint. The  $\pi^0\pi^0$  invariant mass was then calculated from the decay vertex based on the best pairing. The event selections were (1) four reconstructed photons (3×3 cluster algorithm) in the lead-glass (> 10cm separation), (2) cluster shape cut to reduce merged photons from  $3\pi^0$ , (3) photon energy cut  $1.5 \text{ GeV} < E_\gamma < 60 \text{ GeV}$ , (4)  $\gamma$  veto cuts to reject  $3\pi^0$ , (5) kaon energy between 40 to 160 GeV, (6) decay z vertex cut. The  $\pi^0\pi^0$  invariant mass is shown in Fig. 14 for  $K_L$  decays, differentiated from  $K_S$  decays by means of the center of energy (see Fig. 15) of the four photons in the calorimeter. The signal region is between 480 and 516 MeV/c<sup>2</sup>. The residual backgrounds from  $K_L \rightarrow \pi^0\pi^0\pi^0$  decays and neutron interaction in the Pb conversion sheet (from 70% data sample) were  $(0.472 \pm 0.032)\%$ . The  $K_L \rightarrow \pi^0\pi^0\pi^0$  background was small (mainly due to nearly hermetic  $\gamma$  veto coverage) and was well reproduced by a monte carlo simulation. The background was normalized to the data in the decay region 3m upstream of the Pb sheet. The invariant mass for  $K_S$  decays is shown in Fig. 16 with a residual neutron interaction background  $(0.017 \pm 0.003)\%$  from the Pb

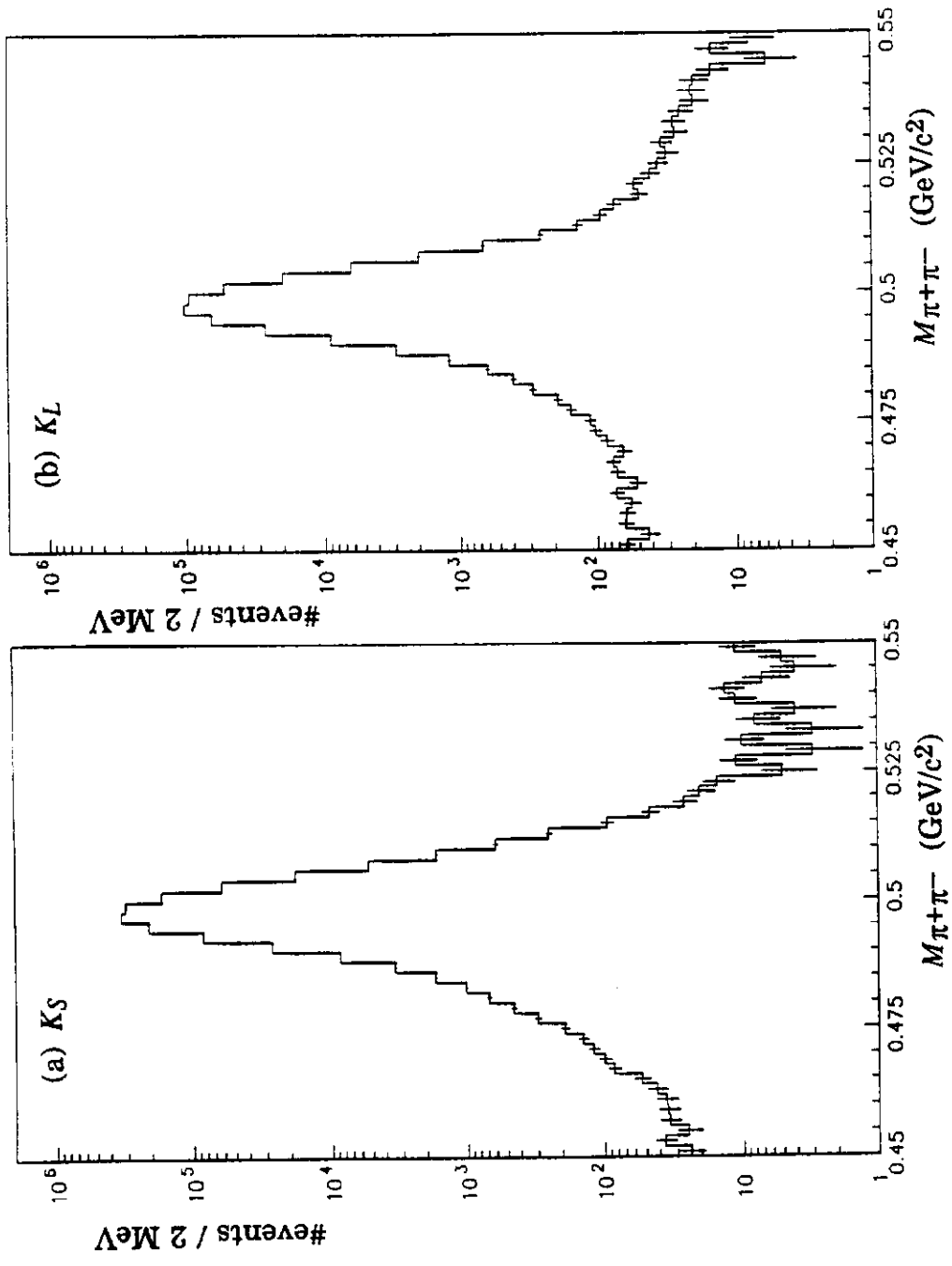


Figure 11: E731  $\pi^+\pi^-$  mass distributions for (a)  $K_S$  and (b)  $K_L$ , full data sample. The mass resolution is 3.5 MeV.

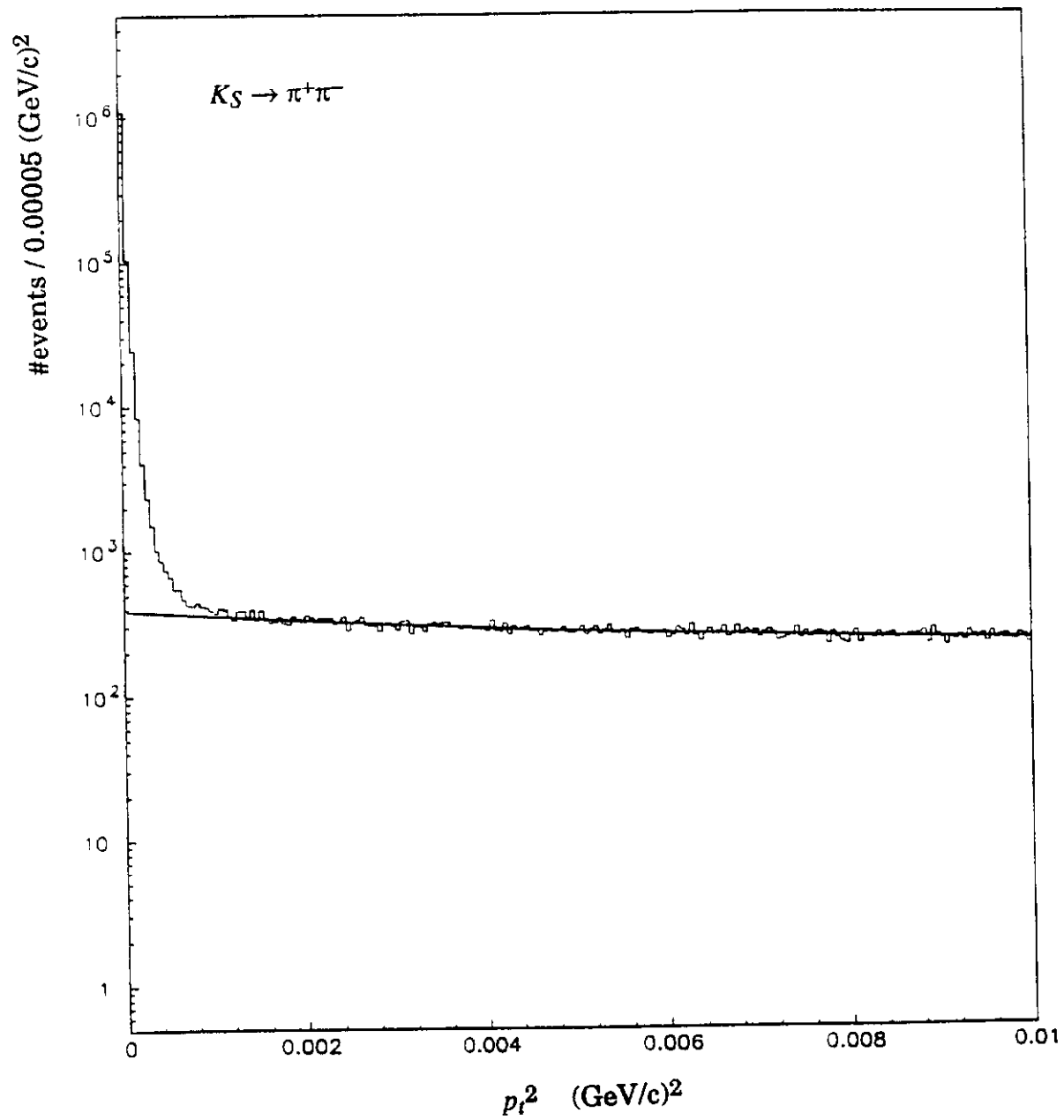


Figure 12: The E731  $K_S \rightarrow \pi^+\pi^- p_t^2$  distribution. The coherent  $K_S$  signal is defined as  $p_t^2 < 0.00025 \text{ (GeV/c)}^2$ , the remaining non-coherent background from the fit amounts to 0.15%.

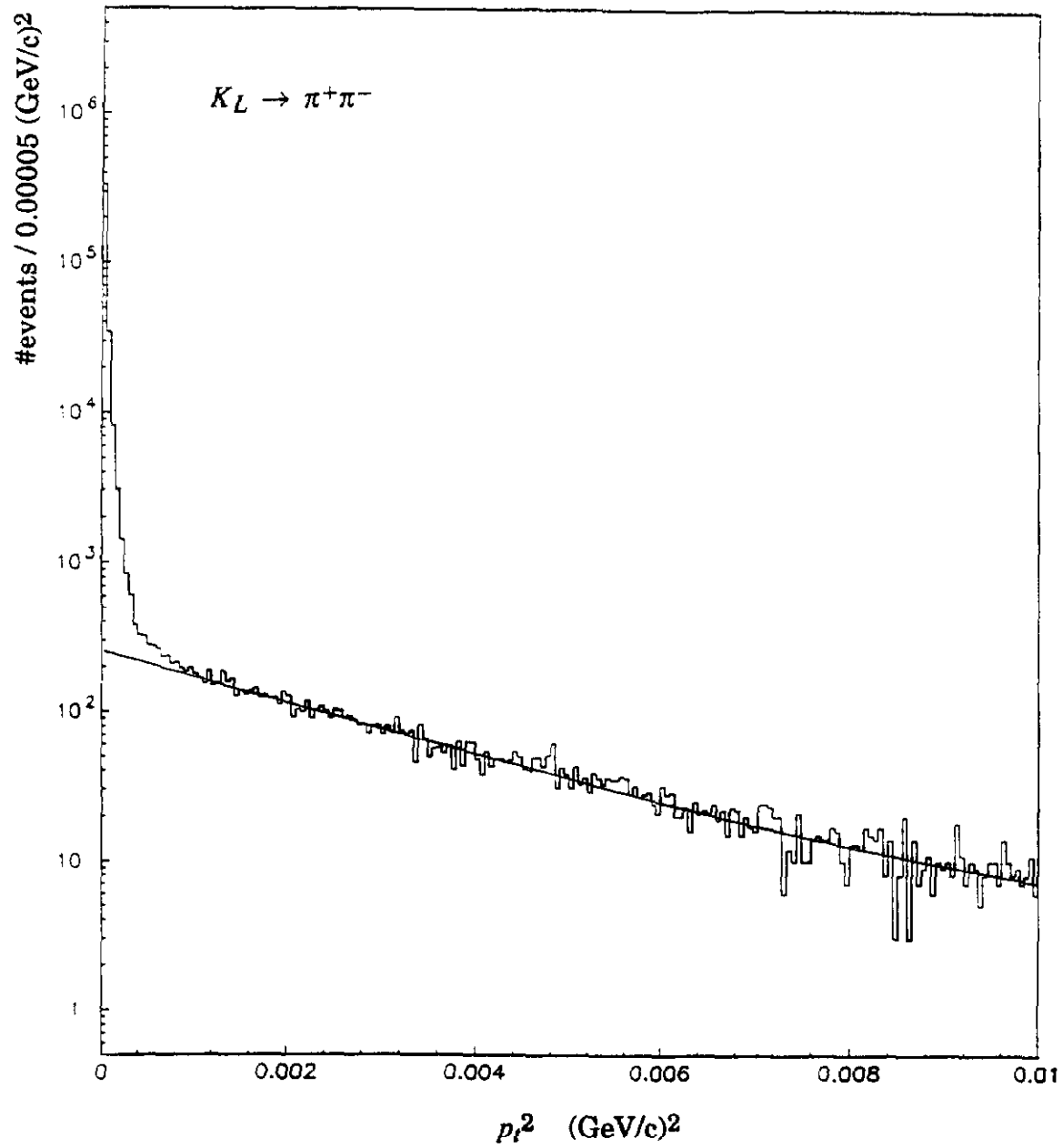


Figure 13: The E731  $K_L \rightarrow \pi^+\pi^-$   $p_t^2$  distribution. The  $K_L$  signal is defined as  $p_t^2 < 0.00025$  (GeV/c)<sup>2</sup>, the remaining semileptonic (mainly  $K_{e3}$ ) background from the fit amounts to 0.339%.

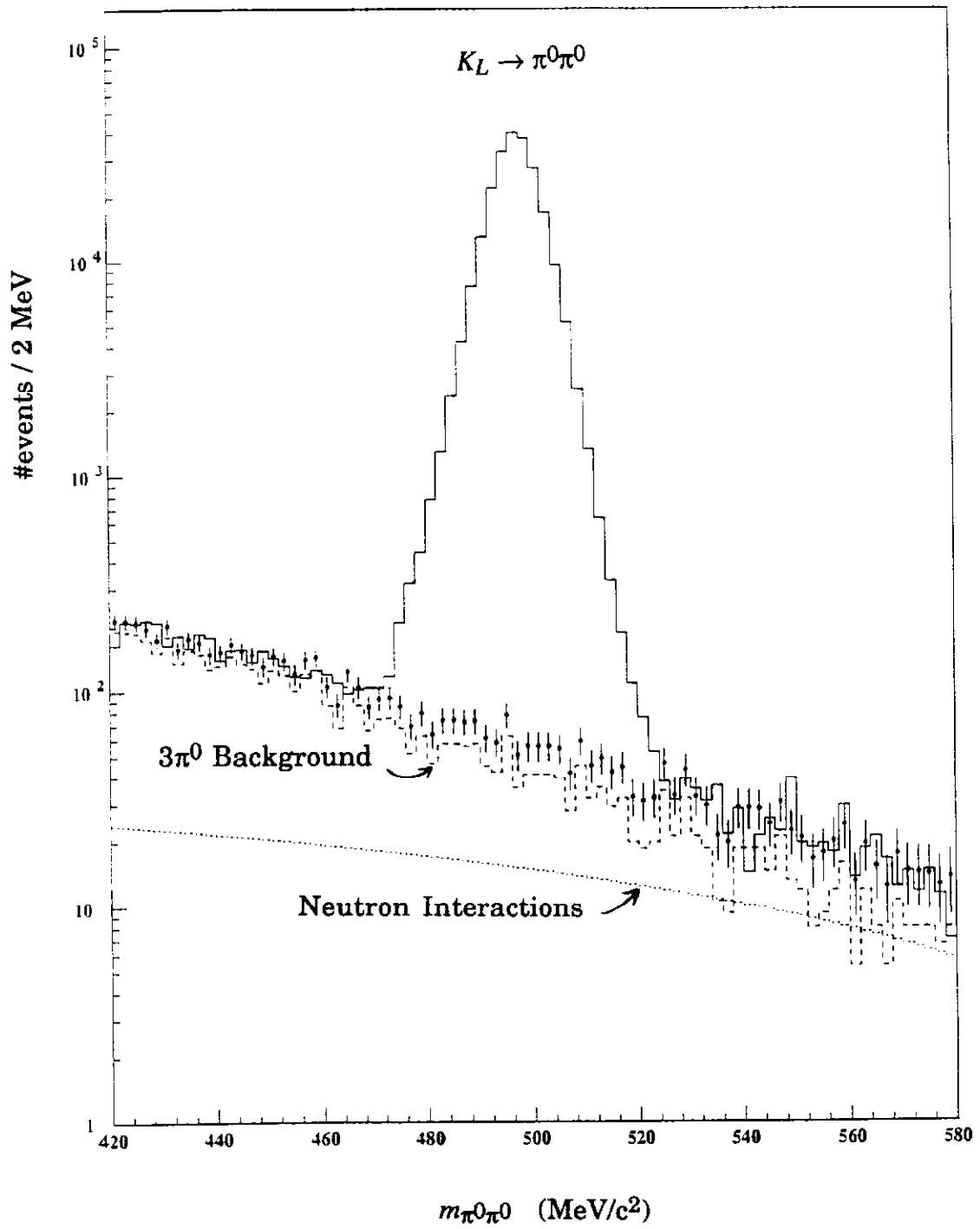


Figure 14: The E731  $K_L \rightarrow \pi^0 \pi^0$  mass distribution with  $3\pi^0$  background (simulated by Monte Carlo) and neutron interaction in the Pb conversion sheet (determined by overall fit) overlaid.

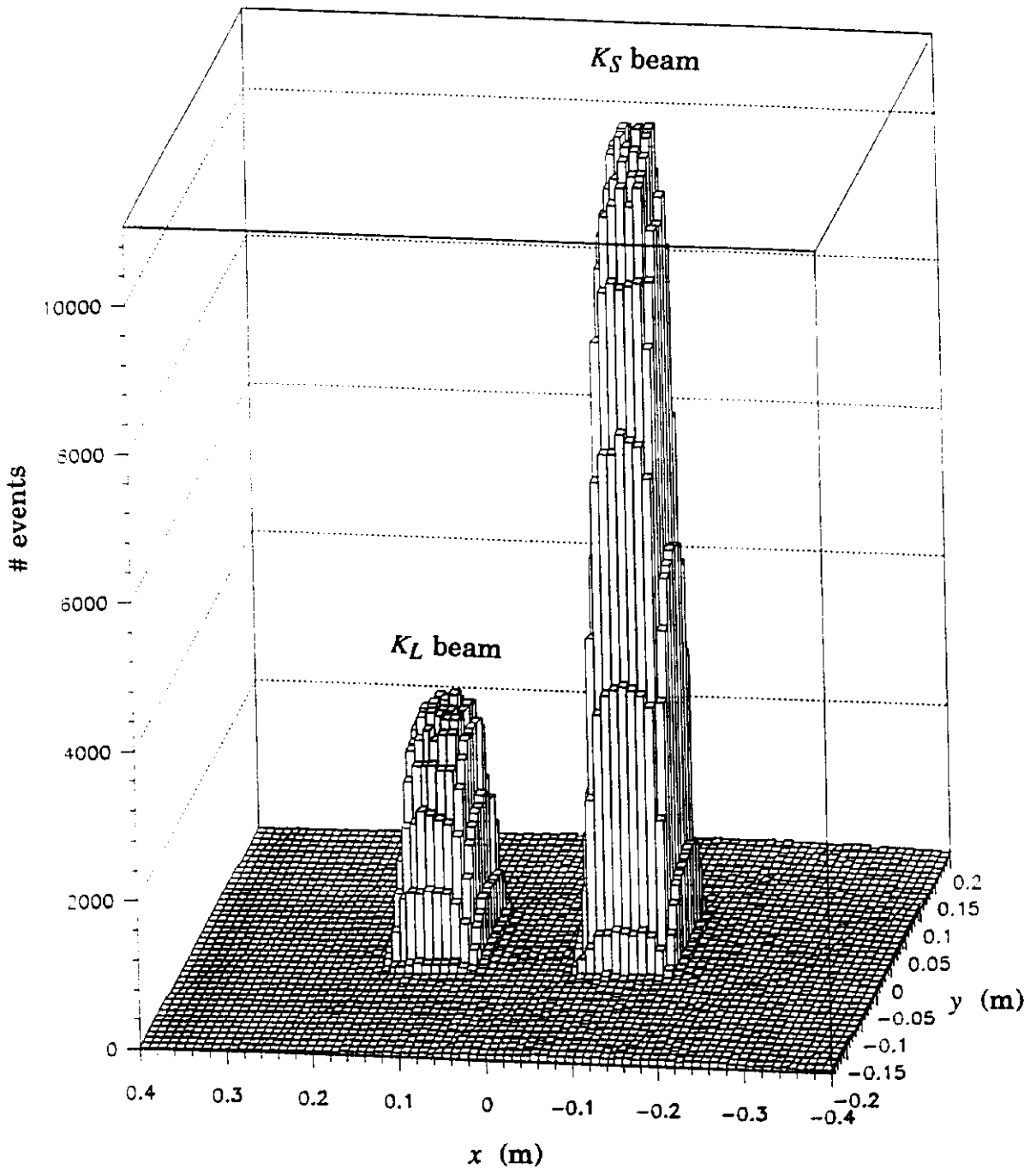


Figure 15: Lego plot of the center of energy distribution at the lead-glass calorimeter in E731. The equal-area box rings drawing from the center of each beam are used to determine the non-coherent background.

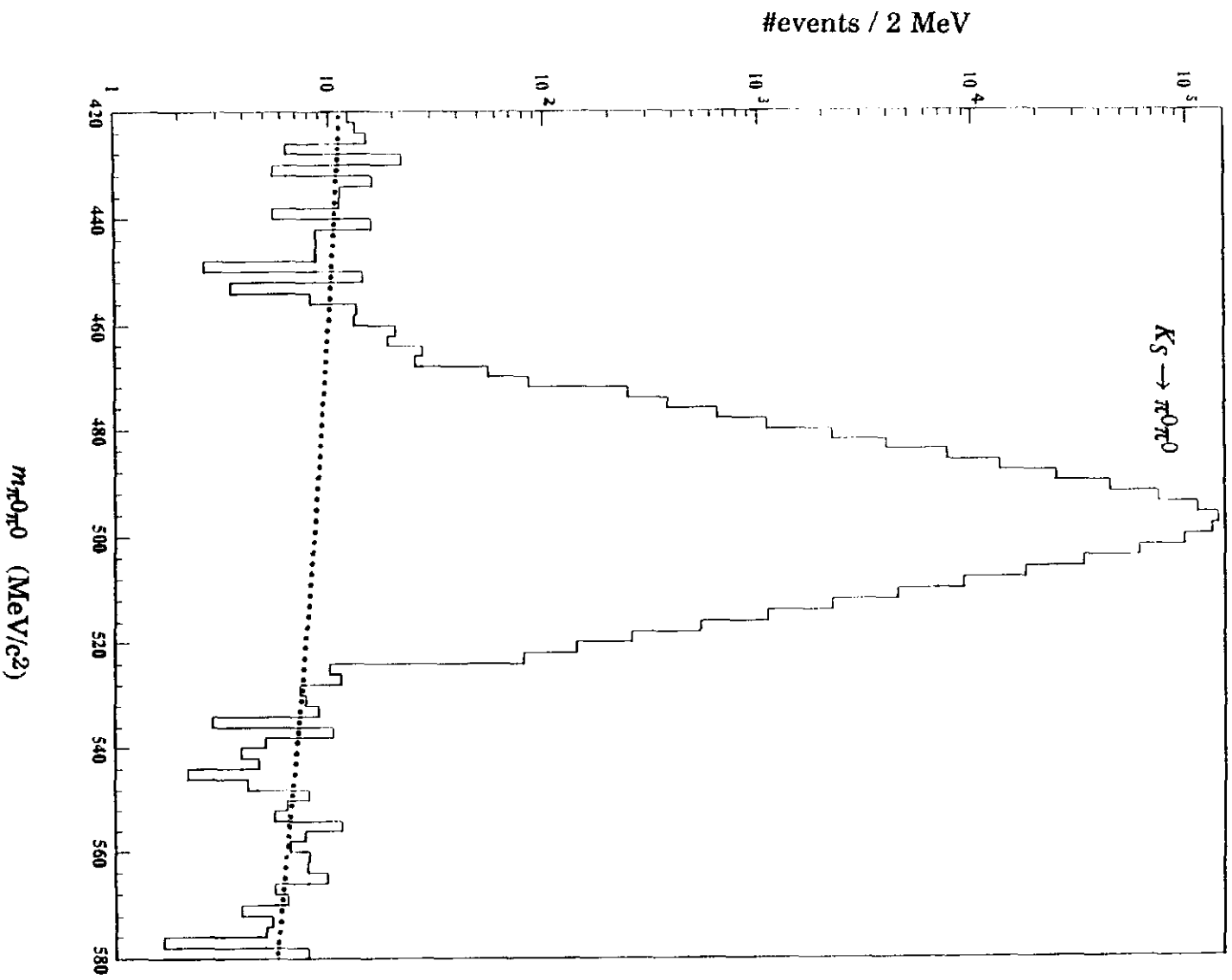


Figure 16: The E731  $K_S \rightarrow \pi^0 \pi^0$  mass distribution with small neutron interaction background in the Pb conversion sheet overlaid.

sheet data. For neutral decays, only the center of energy at the lead-glass was available to identify incoherently regenerated  $K_S$ , which scattered into both vacuum and regenerated beams. Their contributions (the shape of incoherent scattering) were accurately predicted from the  $p_t^2$  distribution of the observed  $K_S \rightarrow \pi^+\pi^-$  decays (as seen in Fig. 12). Figure 17 and 18 shows the size and shape of this prediction agree very well with the observed event density distribution in equal-area concentric box rings around the  $K_L$  and  $K_S$  beams. The background under the coherent beam ( corresponds to a beam area of  $10.6 \text{ cm} \times 10.6 \text{ cm}$ ) was found to be  $[4.27 \pm 0.05(\text{syst})]\%$  for  $K_L$  and  $[2.55 \pm 0.07(\text{syst})]\%$  for  $K_S$ . All backgrounds are summarized in Table 6.

Table 6: Backgrounds summary for E731

| Mode                         | Background process                                 | Background level      |
|------------------------------|--|-----------------------|
| $K_L \rightarrow \pi^+\pi^-$ | Semi-leptonic $K_{e3}$                             | $0.339\% \pm 0.015\%$ |
| $K_S \rightarrow \pi^+\pi^-$ | Non-coherent $K_S$                                 | $0.150\% \pm 0.011\%$ |
| $K_L \rightarrow \pi^0\pi^0$ | $K_L \rightarrow 3\pi^0$ ,<br>neutron interactions | $0.472\% \pm 0.032\%$ |
|                              | Non-coherent $K_S$<br>cross over                   | $4.27\% \pm 0.05\%$   |
| $K_S \rightarrow \pi^0\pi^0$ | neutron interactions                               | $0.017\% \pm 0.003\%$ |
|                              | Non-coherent $K_S$                                 | $2.55\% \pm 0.07\%$   |

An acceptance correction is necessary, primarily to deal with the simple geometrical fact that  $K_S$  and  $K_L$  decay vertex distributions are different. This is done with a detailed Monte Carlo simulation of the beam and detector. The detector parameters and aperture locations were taken from direct measurements and analysis of high statistics  $K_{e3}$  and  $3\pi^0$  sample. Same  $K_L$  momentum spectra parametrization was used for all data set. The tunable parameters were neutral beam collimator positions and targeting angles, determined set by set by matching

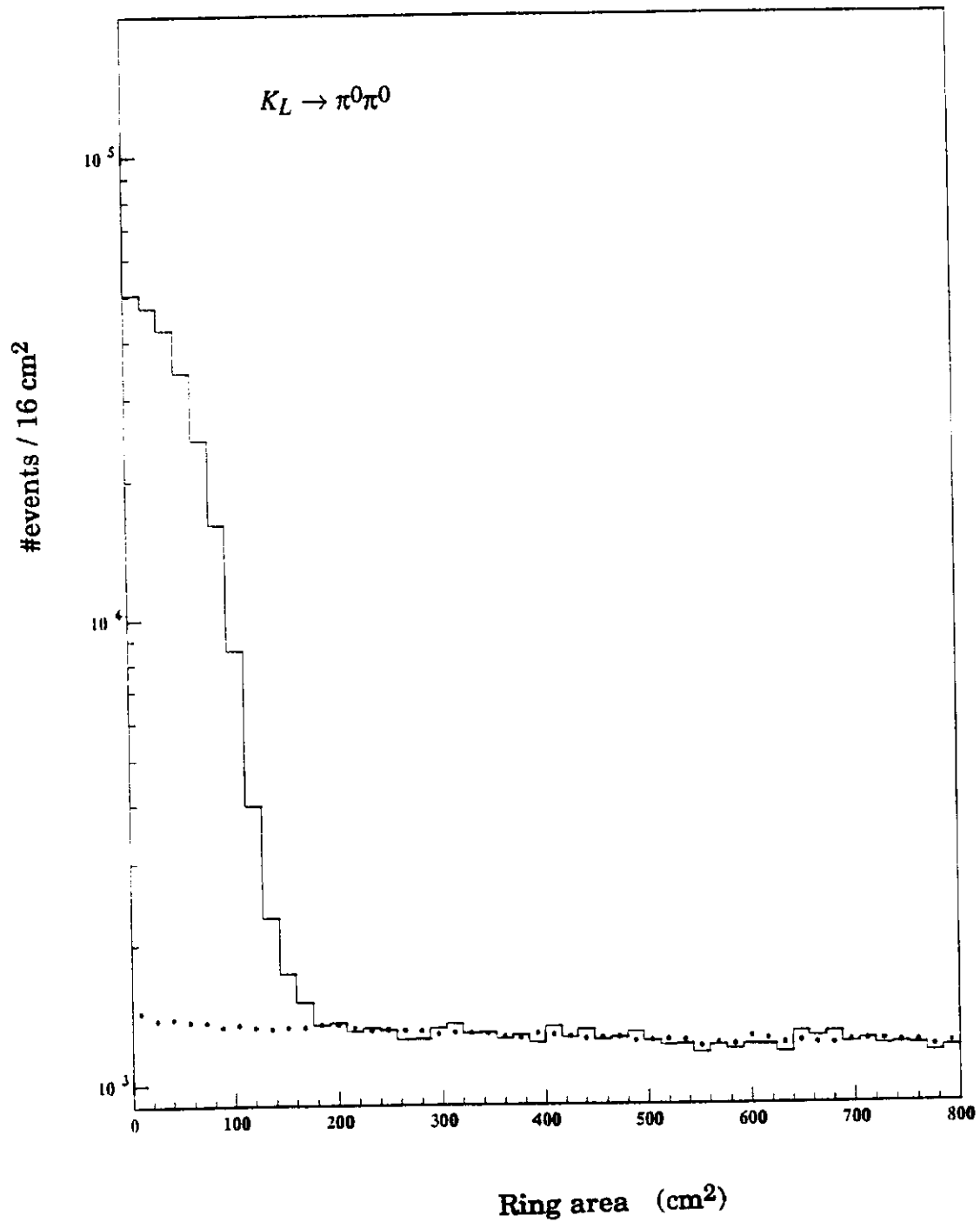


Figure 17: The event density in equal-area concentric box rings around the  $K_L$  beam. The solid circles show the expected size and shape of the "cross-over" incoherent background from the regenerator as determined from  $\pi^+ \pi^-$ .

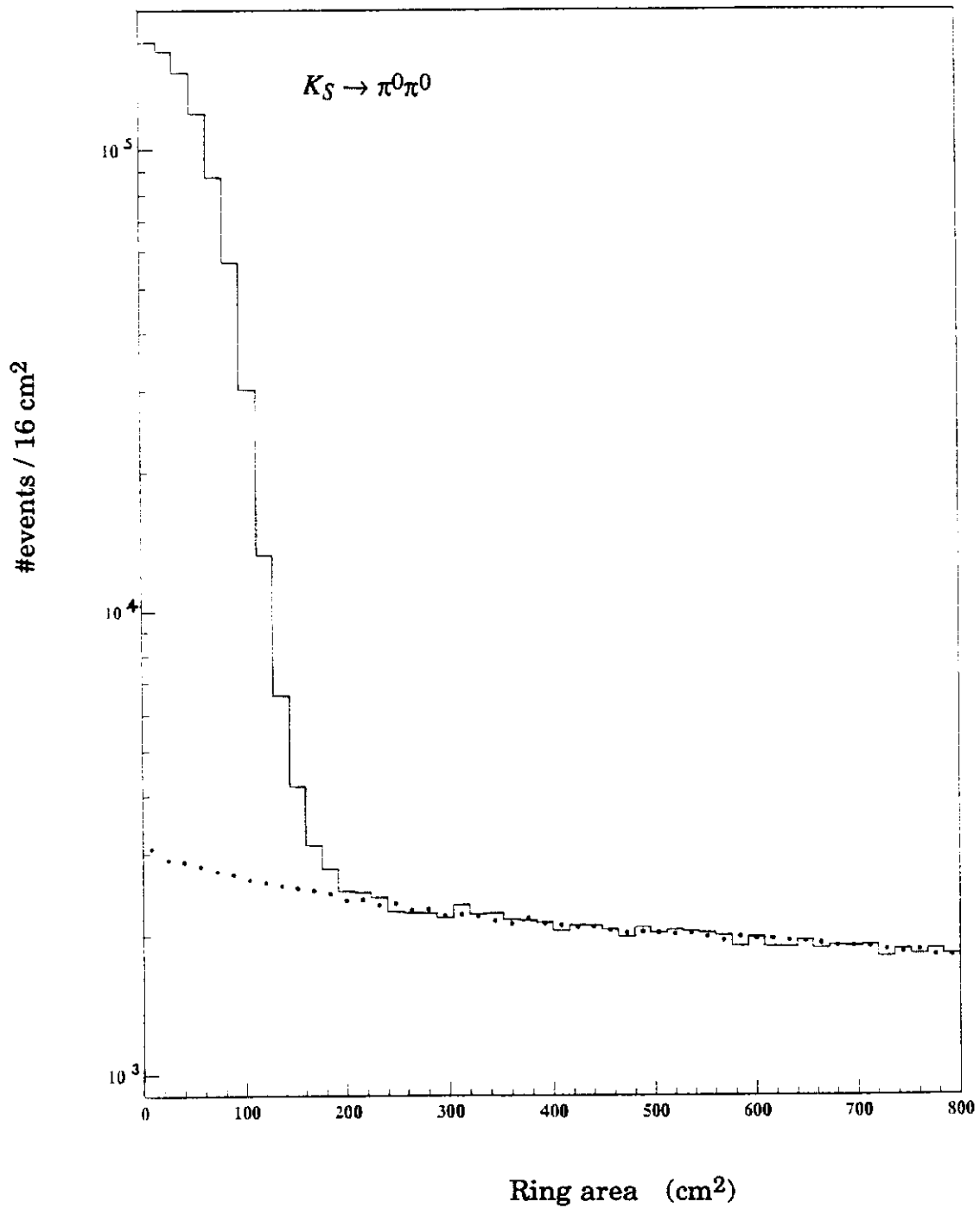


Figure 18: The event density in equal-area concentric box rings around the  $K_S$  beam. The solid circles show the expected size and shape of the diffractive and inelastic background from the regenerator as determined from  $\pi^+\pi^-$ .

data with Monte Carlo simulation. The final result is not particularly sensitive to them.

The nonlinearity and non-Gaussian response of the lead-glass to electrons and photons, affecting the vertex reconstruction in neutral decays, were reproduced with no free parameters, by using the results from EGS simulations together with the effective attenuation length of Cherenkov light in each block obtained from the calibration data. For the last 25% data sample, when all four modes were collected simultaneously, the requirement that the *same* detector and beam parameters be used in the simulation for all four modes provided a powerful check to the Monte Carlo simulation as a whole. The  $K_L \rightarrow \pi^+\pi^-$  decay-vertex distribution is well reproduced by the Monte Carlo simulation, as shown in Fig. 19. The agreement is equally good for the  $K_S \rightarrow \pi^+\pi^-$ , as seen in Fig. 20, as well as for  $K_{L,S} \rightarrow \pi^0\pi^0$  in Fig. 21 and Fig. 22.

The final data sample included kaons with energy between 40 and 160 GeV decaying in the region from 110 to 137 m from the target. The raw number of events passing all cuts are given in Table 7. The acceptance was similar for  $K_S$  and  $K_L$ : It varied slowly with decay vertex, the mean of which differed for  $K_S$  and  $K_L$  decays by less than 1.5 m. The total change in the double ratio from raw data to final background and acceptance corrected samples is about 7%.

Table 7: E731 full data sample statistics used in this analysis.

| Mode                         | # events  |
|------------------------------|-----------|
| $K_L \rightarrow \pi^0\pi^0$ | 223,994   |
| $K_S \rightarrow \pi^0\pi^0$ | 775,197   |
| $K_L \rightarrow \pi^+\pi^-$ | 330,151   |
| $K_S \rightarrow \pi^+\pi^-$ | 1,062,319 |

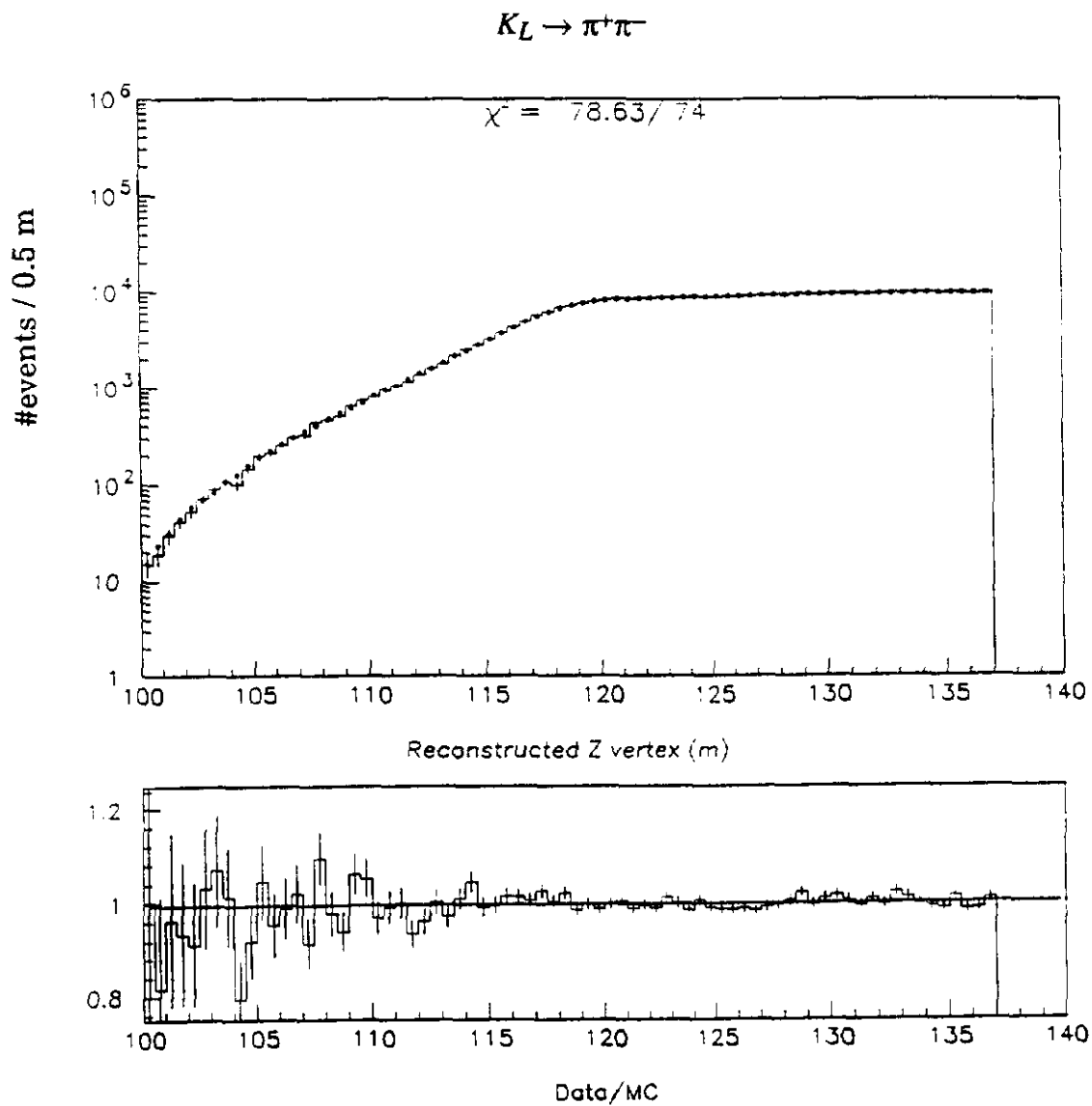


Figure 19: The E731 decay z-vertex distribution for  $K_L \rightarrow \pi^+\pi^-$  events. The histogram is data and the solid circles are from a Monte Carlo simulation. Lower plot is the ratio of data divided by Monte Carlo. The Monte Carlo is used for acceptance correction.

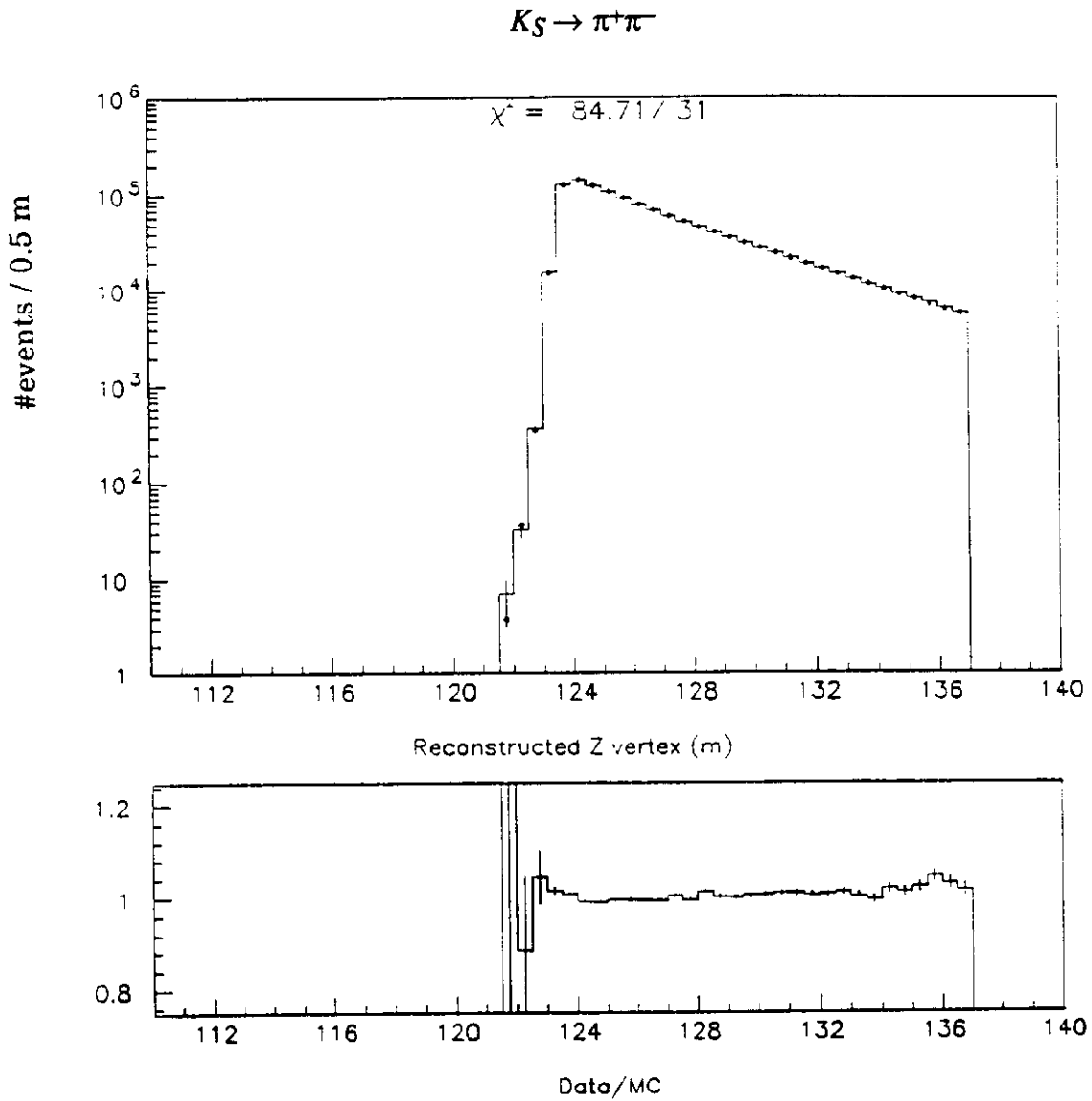


Figure 20: The E731 decay z-vertex distribution for  $K_S \rightarrow \pi^+\pi^-$  events. The histogram is data and the solid circles are from a Monte Carlo simulation. Lower plot is the ratio of data divided by Monte Carlo.

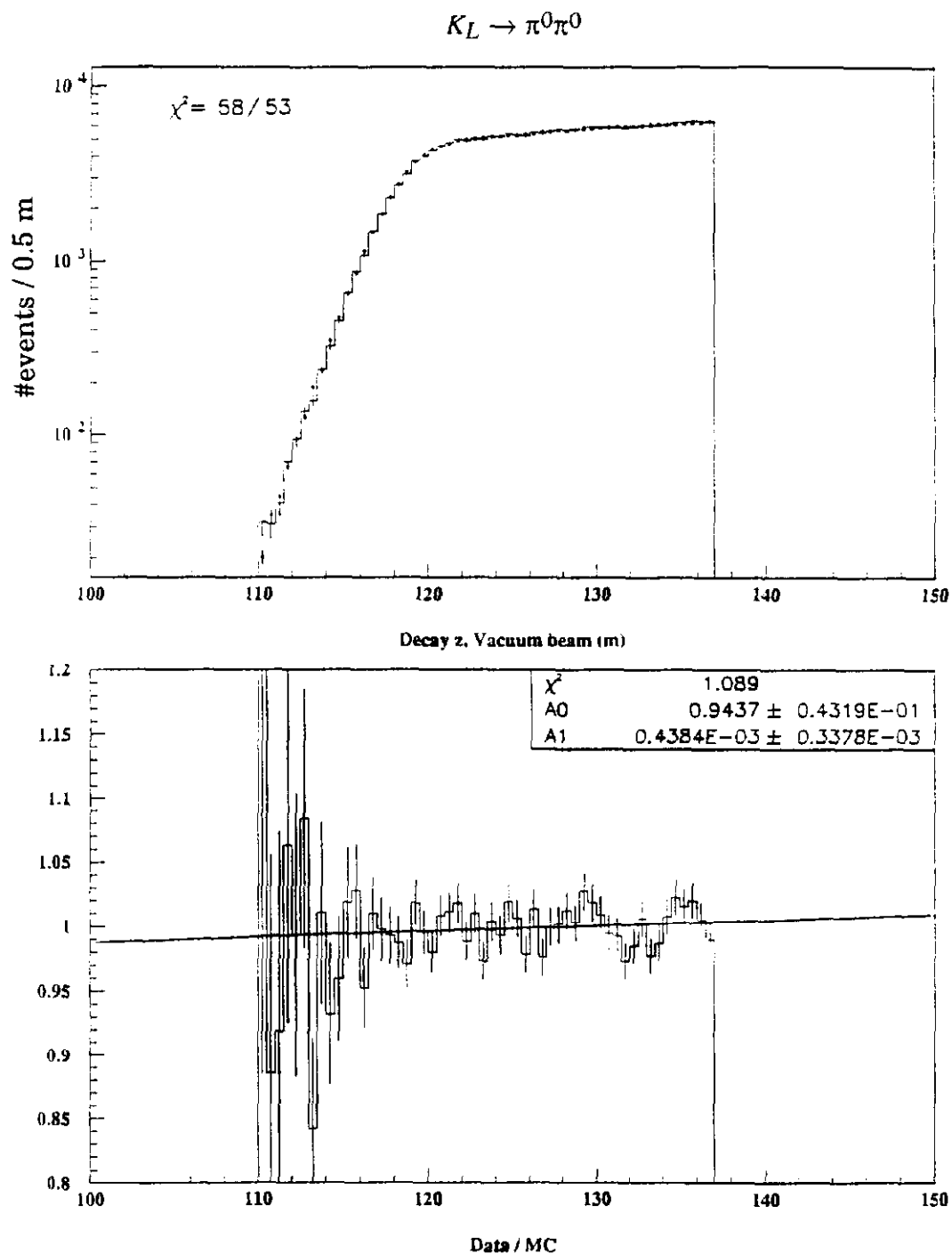


Figure 21: The E731 decay z-vertex distribution for  $K_L \rightarrow \pi^0\pi^0$  events. The histogram is data and the solid circles are from a Monte Carlo simulation. Lower plot is the ratio of data divided by Monte Carlo.

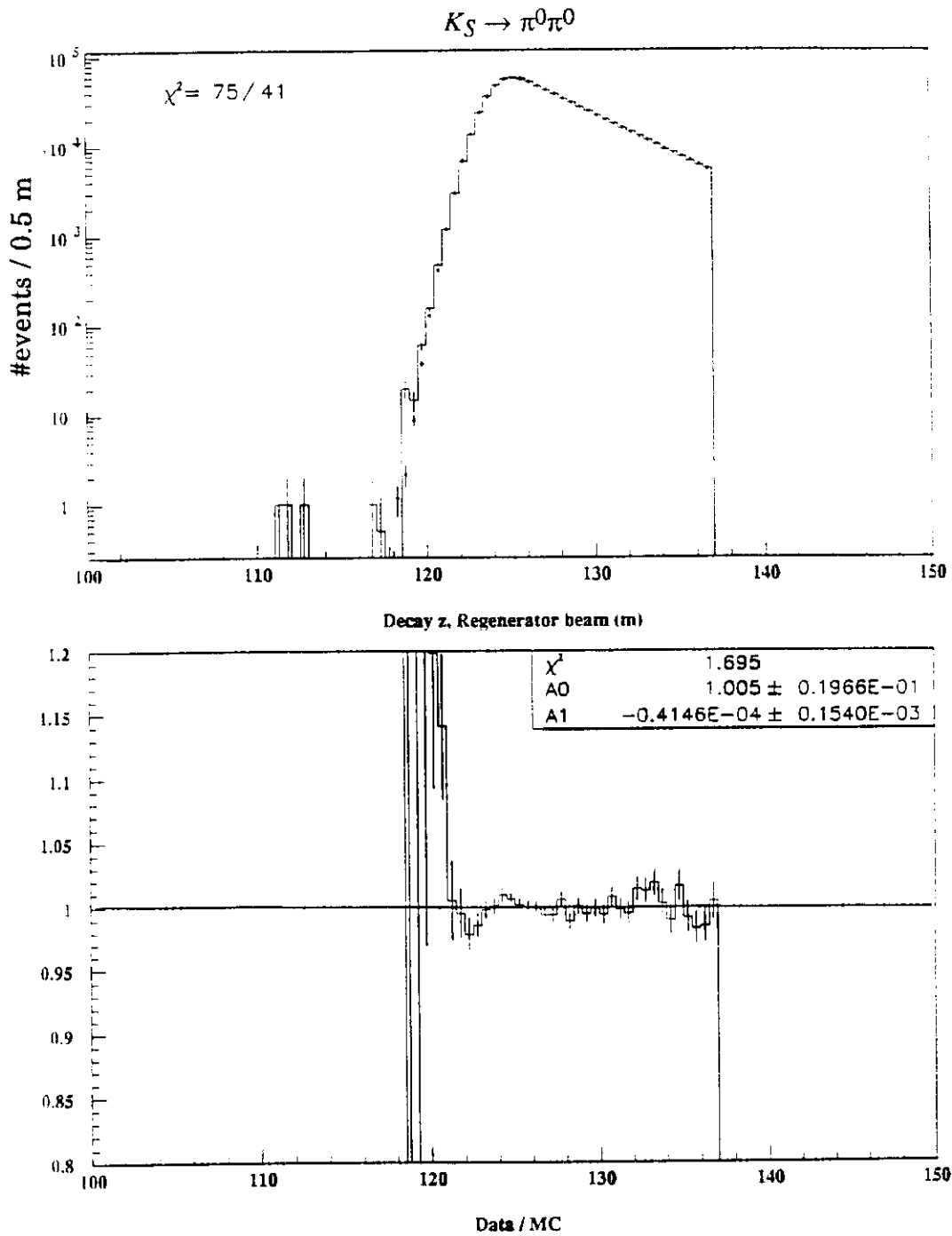


Figure 22: The E731 decay z-vertex distribution for  $K_S \rightarrow \pi^0 \pi^0$  events. The histogram is data and the solid circles are from a Monte Carlo simulation. Lower plot is the ratio of data divided by Monte Carlo.

## THE E731 RESULTS

To extract  $Re(\epsilon'/\epsilon)$ , we fit  $R_{+-}$  and  $R_{00}$  for  $|\rho/\eta|$  in the two modes in 10 GeV/c kaon momentum bins. The momentum dependence, common to the neutral and charged modes, is expected to obey a power law,<sup>12)</sup>  $p^\alpha$ , while a magnitude difference is proportional to  $Re(\epsilon'/\epsilon)$ . Figure 23 and Fig. 24 show the fitted power law dependence for  $|\rho/\eta|$ . The best-fit power  $\alpha$  for the charged (neutral) mode was  $-0.602 \pm 0.004$  ( $-0.603 \pm 0.005$ ) with  $\chi^2 = 10.1$  (10.4) for 10 degrees of freedom. The two values are consistent with each other and with previous determinations.<sup>13)</sup> The combined fit yielded  $Re(\epsilon'/\epsilon) = +0.00060 \pm 0.00058(\text{stat}) \pm 0.00018(\text{MC})$ , where the first error came from data statistics and the second error from Monte Carlo statistics. The Monte Carlo statistics was about 6 times the data statistics for neutral mode and 9 times for charged mode. Reanalysis of the 20% data sample used in the previous publication with improved calibration, alignment, and background studies, gives  $Re(\epsilon'/\epsilon) = (-1 \pm 14(\text{stat.})) \times 10^{-4}$ , in good agreement with the published value.<sup>7)</sup>

Systematic errors were associated with background subtractions, accidental activity in the detector, energy calibration and resolution, and acceptance. The systematic errors are summarized in Table 8.

Uncertainty in the backgrounds was dominated by those in the incoherent contributions to neutral decays, which are expected to partially cancel in  $R_{00}$ . As a conservative estimate of the total uncertainty on the double ratio  $R$ , all background errors were added in quadrature, yielding a total of 0.10%. All decays to a common final states were analyzed together, this and the use of loose cuts (the reconstruction efficiency was more than 90%) greatly reduced sensitivity to time variations. Therefore  $R_{+-}$  and  $R_{00}$  were stable throughout the run, even though the intensity, targeting, and detector efficiencies varied. A check on this is to plot the fitted regeneration amplitude at 70 GeV *verses* various data sets throughout the whole run for  $\pi^+\pi^-$  data and  $\pi^0\pi^0$  data respectively (see Fig. 25), when  $\eta$  has been fixed in the fit.

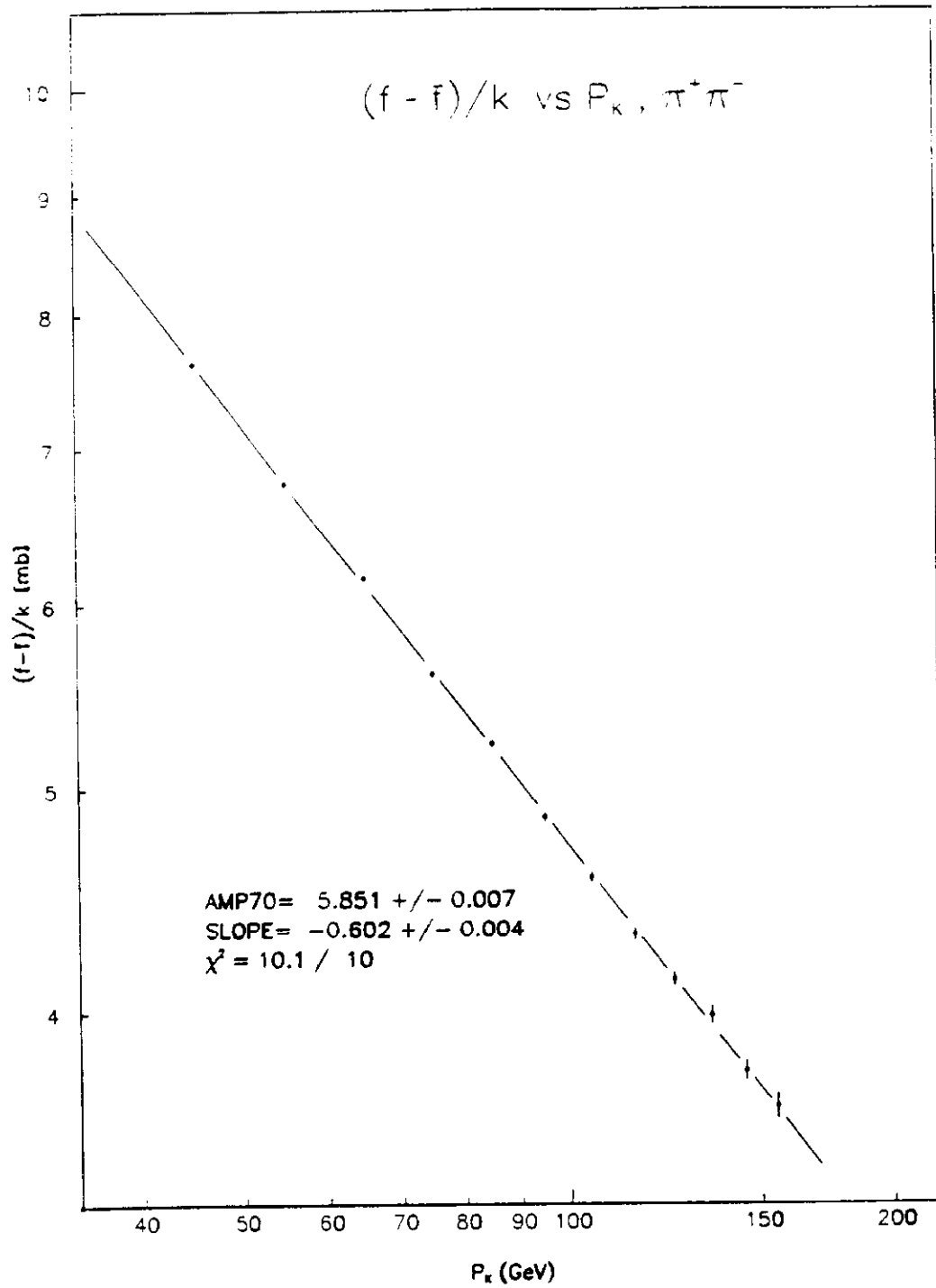


Figure 23: The fit of  $|\rho/\eta|$  versus kaon momentum for  $\pi^+\pi^-$  mode.

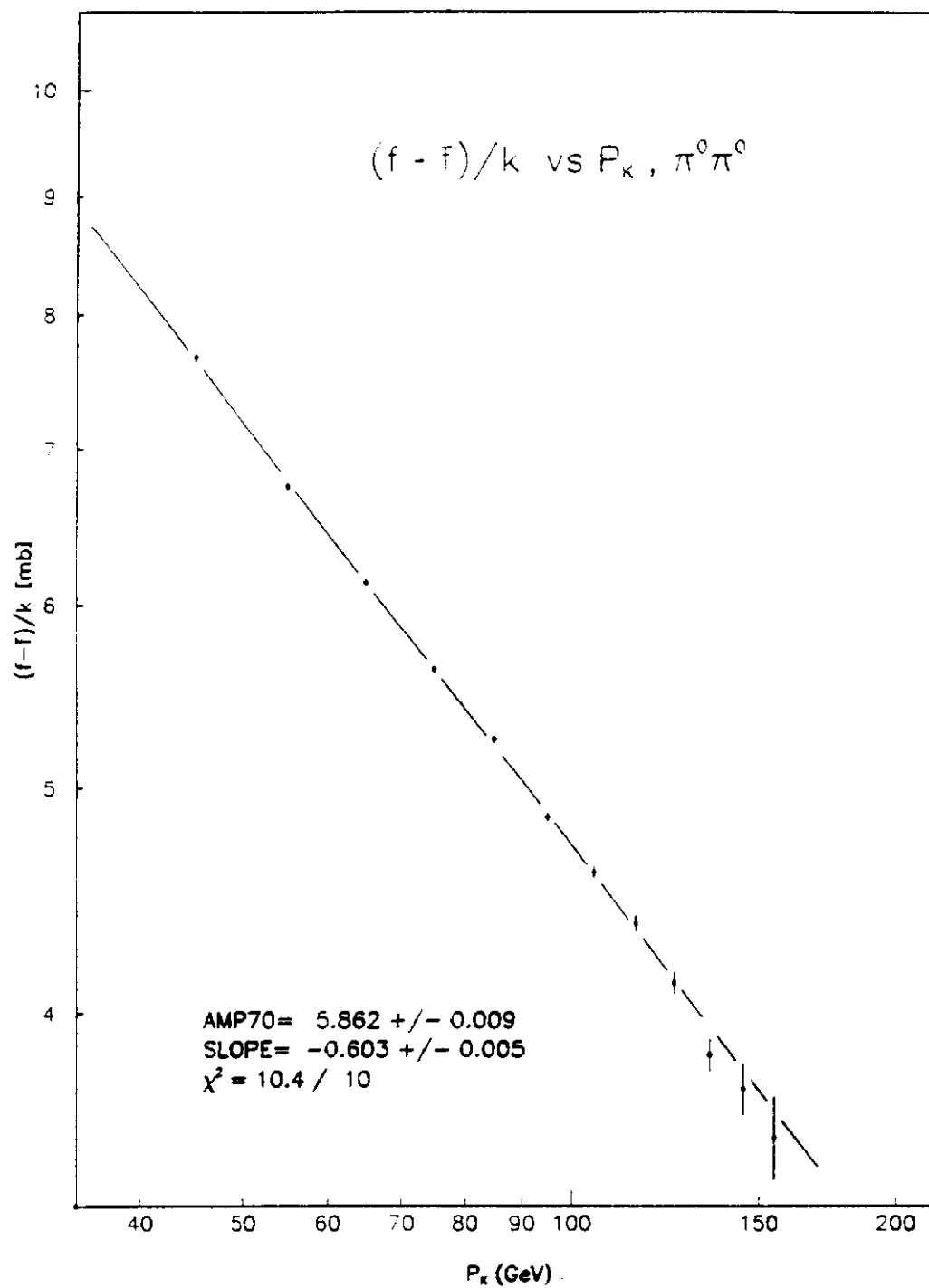


Figure 24: The fit of  $|\rho/\eta|$  versus kaon momentum for  $\pi^0\pi^0$  mode.

# 70 GeV/c AMPLITUDES

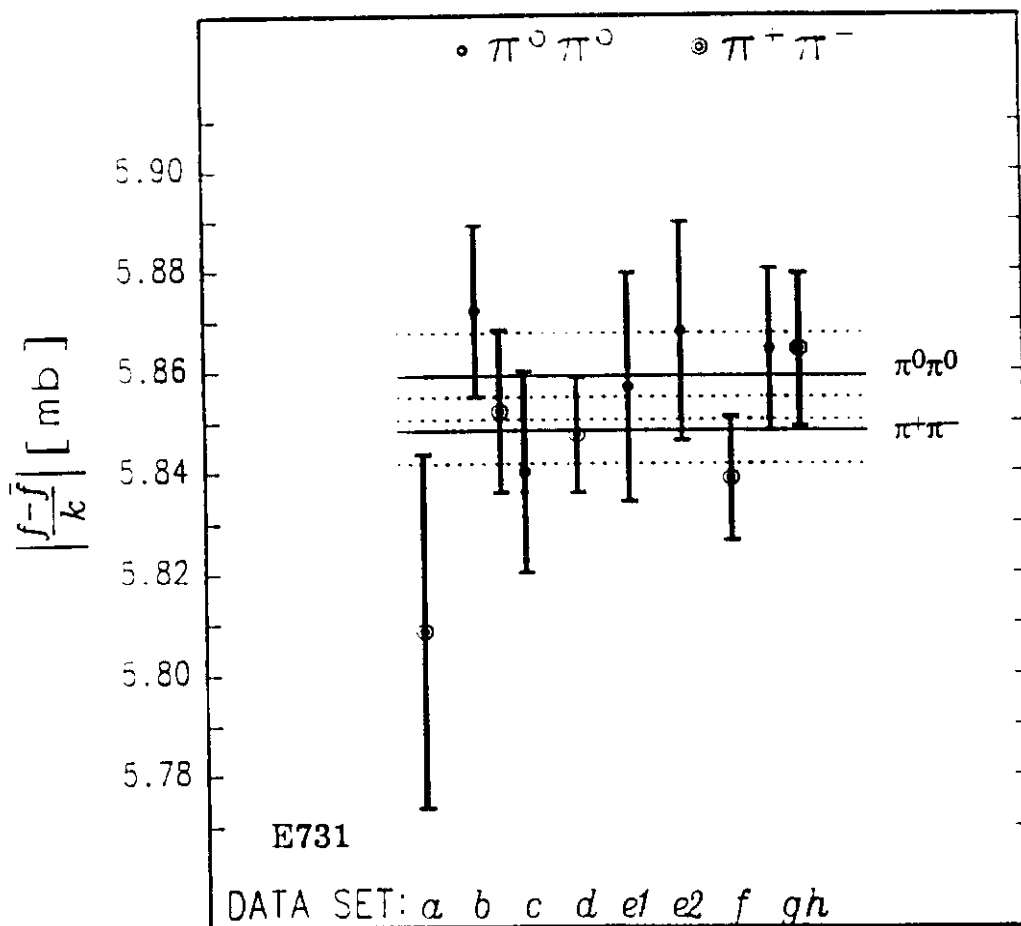


Figure 25: The fitted regeneration amplitude at 70 GeV *verses* data sets for  $\pi^+ \pi^-$  and  $\pi^0 \pi^0$  data. A check on the single ratio stability *verses* time.

The averages for charged and neutral data are within one sigma (errors overlap each other), indicate a very small  $\epsilon'/\epsilon$ .

Table 8: E731 systematic errors on double ratio  $R$ .

| <i>Systematics</i>            | <i>Sources</i>  | <i>Systematic error to R</i> | <i>Total error in quadrature</i> |
|-------------------------------|---|------------------------------|----------------------------------|
| Backgrounds                   | $K_L \rightarrow \pi^+\pi^-$                            | 0.015%                       | 0.10%                            |
|                               | $K_S \rightarrow \pi^+\pi^-$                            | 0.011%                       |                                  |
|                               | $K_L \rightarrow \pi^0\pi^0$<br>( $3\pi^0$ and neutron) | 0.032%                       |                                  |
|                               | $K_S \rightarrow \pi^0\pi^0$<br>(neutron)               | 0.003%                       |                                  |
|                               | $K_{L,S} \rightarrow \pi^0\pi^0$<br>(incoherent)        | 0.09%                        |                                  |
| Acceptance                    | charged   | 0.05%                        | 0.11%                            |
|                               | neutral   | <0.10%                       |                                  |
| Calibration                   | charged z-scale   | 0.01%                        | 0.10%                            |
|                               | neutral energy scale                                    | 0.10%                        |                                  |
|                               | neutral resolution                                      | 0.01%                        |                                  |
| Accidentals                   | charged   | 0.04%                        | 0.06%                            |
|                               | neutral   | 0.05%                        |                                  |
| Total systematic error to $R$ |   |                              | 0.19%                            |

Accidental activity, concentrated more near the vacuum beam, could have changed the relative  $K_L$  and  $K_S$  efficiencies. Accidental events, collected with  $\pi\pi$  data at a rate proportional to the instantaneous beam intensity, contained a photon cluster 2%-5% of the time and an average of 4-8.5 chamber hits (depend on intensity). When overlaid on the  $\pi\pi$  Monte Carlo events they correctly reproduced the intensity dependence of our selection criteria. However, little bias between  $K_L$  and

$K_S$  was seen in neutral mode, which changed the ratio  $R_{00}$  by  $0.09\% \pm 0.05\%$  within the statistical error of the simulation. Two effects were dealt with. First, an accidental cluster landing on top of a good one causes the event to be lost most of the time; second, an accidental cluster of low enough energy can hide underneath a good one in a event that causes  $\sim 0.1\%$  total energy shift and  $\sim 6\text{cm}$   $z$  vertex shift on the average. The 1.5 sigma residual effect in the neutral mode after the energy adjustment as in the data, was included in the above result. No shift was observed in the charged ratio  $R_{+-}$  within the statistical error  $\pm 0.04\%$ .

The energy scale accuracy for the charged mode was determined sufficiently using the known  $K^0$  and  $\Lambda$  masses. The charged mode  $z$ -scale was known to  $\sim 6\text{mm}$ , leaving a very small residual uncertainty of 0.01% in  $R_{+-}$ . For the neutral mode, the overall scale was adjusted ( $\approx 0.5\%$ ) using the sharp rising edge in the  $K_S$  decay vertex at the regenerator, leaving a residual uncertainty of 0.10% in  $R_{00}$ . This was done by shifting the neutral mode energy scale by 0.05%, corresponding to 3cm shift in the regenerator  $z$ -edge, a noticeable mismatch was seen in the data *verses* Monte Carlo overlay ( $\chi^2/\text{d.o.f.}$  jumped from 1 to 3). The uncertainty due to energy resolution ( $\sim \pm 1\%$ ) led to a small 0.01% uncertainty in  $R_{00}$ .

Acceptances were extensively studied using high statistics  $\pi e \nu$  and  $\pi^0 \pi^0 \pi^0$  decays taken with the  $\pi\pi$  events. The agreement in vertex, momentum and other distributions with Monte Carlo simulation over the fiducial region was excellent. Typically, the critical apertures were determined to within  $100\mu\text{m}$ . Figure 26 shows the data *verses* Monte Carlo overlay on the  $z$ -vertex distribution for  $3\pi^0$  data (no lead sheet data), an excellent agreement. Also, when  $Re(\epsilon'/\epsilon)$  was extracted using small vertex bins (eliminating the need for acceptance corrections), a consistent result was obtained. These studies, together with the stability of  $R_{+-}$  and  $R_{00}$  when selection criteria, beam profiles and detector apertures and efficiencies were varied in the Monte Carlo simulation, led us to assign 0.05% systematic uncertainty for charged mode and  $< 0.10\%$  uncertainty for neutral mode due to acceptance.

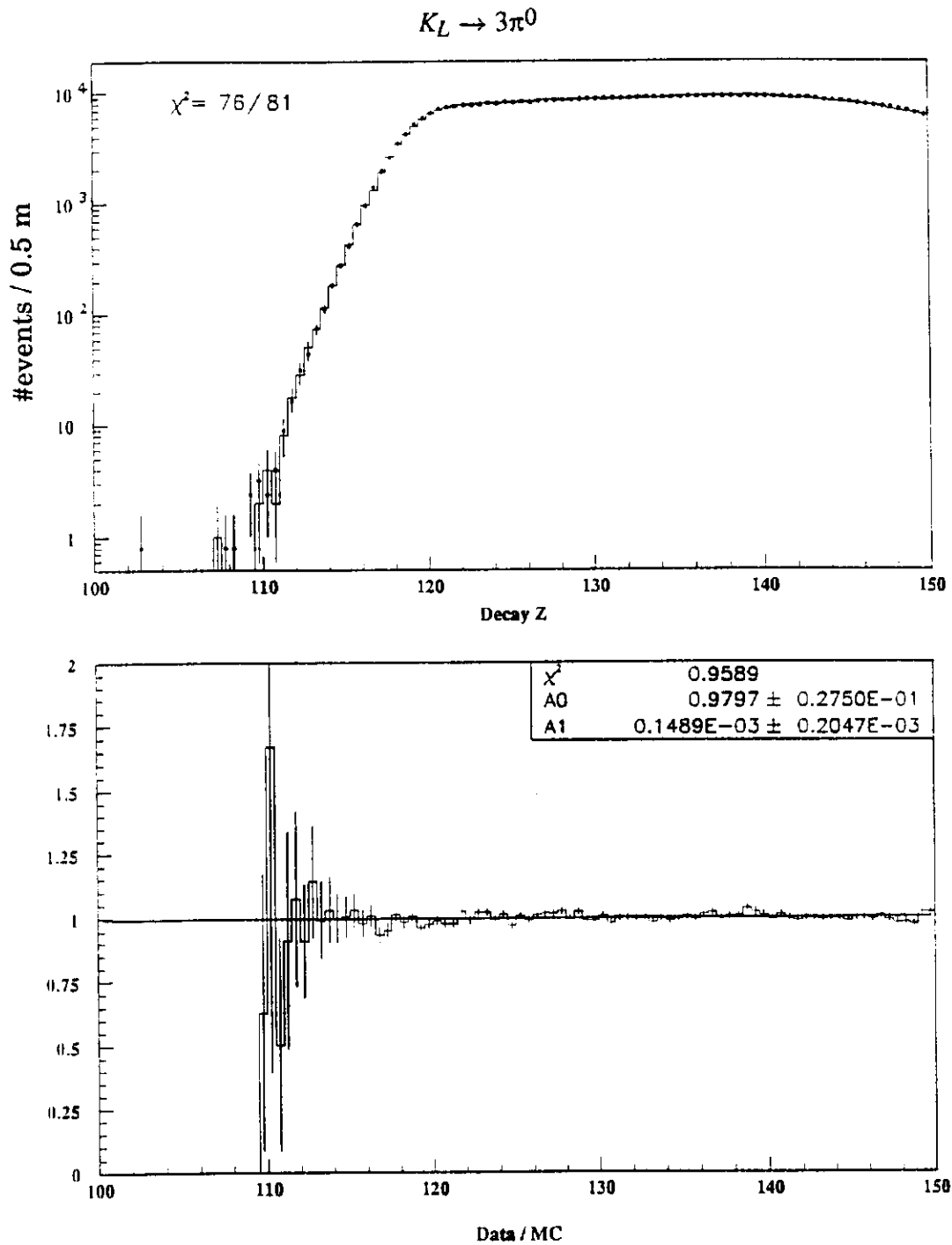


Figure 26: The E731  $K_L \rightarrow 3\pi^0$  decay z-vertex distribution (data sets with no Pb conversion sheet). The histogram is data and the closed circles are from the Monte Carlo simulation. A check on the neutral mode acceptance.

Combining these uncertainties in quadrature, the total systematic error on the double ratio is then  $\pm 0.19\%$ , corresponding to a systematic error on  $\text{Re}(\epsilon'/\epsilon)$  of  $\pm 3.2 \times 10^{-4}$ , a factor of 2 improvements over the previous published 20% data sample. The final *preliminary* result is

$$\text{Re}(\epsilon'/\epsilon) = (6.0 \pm 5.8(\text{stat.}) \pm 3.2(\text{syst.}) \pm 1.8(\text{MC})) \times 10^{-4}$$

or, with all errors combined in quadrature,

$$\text{Re}(\epsilon'/\epsilon) = (6.0 \pm 6.9) \times 10^{-4}. \quad (\text{E731 preliminary full data})$$

This result is still consistent with the Superweak model, i.e.  $\epsilon'/\epsilon = 0$ ; it does not confirm the NA31's result,  $(23 \pm 7) \times 10^{-4}$ . The total error of the E731 full data sample is still dominated by the statistical error with a much reduced systematic error.

The same  $2\pi$  data have also been fitted for other parameters in the neutral kaon system, using exactly the same techniques of background subtraction and acceptance corrections. The results, where both statistical and systematic errors were included, are

$$\tau_S = (0.8912 \pm 0.0013) \times 10^{-10} \text{ sec};$$

$$\Delta m = m_L - m_S = (0.5339 \pm 0.0034) \times 10^{10} \hbar \text{ sec}^{-1};$$

$$\phi_{+-} = (43.2 \pm 1.6)^\circ;$$

$$\Delta\phi = \phi_{00} - \phi_{+-} = (-0.6 \pm 1.6)^\circ;$$

$$\phi_{SW} = \tan^{-1} \left[ \frac{2\Delta m}{\Gamma_S} \right] = (43.37 \pm 0.22)^\circ.$$

These results are either comparable to or exceed in precision the best previous determinations. Detailed comparison of the fitted results for both charged and neutral modes with the best previous measurements are listed in Table 9.

Table 9: Other fitted results from the same E731  $2\pi$  data sample.

| A. Fits to the $K_S$ lifetime $\tau_S$ [ $10^{-10}$ sec] (assuming CPT) |                     |                 |                 |                  |
|---|---------------------|-----------------|-----------------|------------------|
|   | $\tau_S$ result     | stat. error     | syst. error     | total error      |
| E731 $\pi^+\pi^-$ data<br>(preliminary)                                 | 0.8912              | $\pm 0.0012$    | $\pm 0.0006$    | $\pm 0.0013$     |
| E731 $\pi^0\pi^0$ data<br>(preliminary)                                 | 0.8952              | $\pm 0.0016$    | $\pm 0.0032$    | $\pm 0.0036$     |
| Best previous<br>measurement: <sup>14)</sup><br>Carithers <i>et al.</i> | 0.8913              |                 |                 | $\pm 0.0032$     |
| PDG average <sup>15)</sup>  | 0.8922              |                 |                 | $\pm 0.0020$     |
| B. Fits to $\Delta m$ [ $10^{10}$ h/sec] (assuming CPT)                 |                     |                 |                 |                  |
|   | $\Delta m$ result   | stat. error     | syst. error     | total error      |
| E731 $\pi^+\pi^-$ data<br>(preliminary)                                 | 0.5339              | $\pm 0.0031$    | $\pm 0.0015$    | $\pm 0.0034$     |
| E731 $\pi^0\pi^0$ data<br>(preliminary)                                 | 0.5353              | $\pm 0.0053$    | $\pm 0.0037$    | $\pm 0.0065$     |
| Best previous<br>measurement: <sup>16)</sup><br>Geweniger <i>et al.</i> | 0.5340              | $\pm 0.0026$    | $\pm 0.0015$    | $\pm 0.0030$     |
| PDG average   | 0.5351              |                 |                 | $\pm 0.0024$     |
| C. Fits for $\phi_{SW}$ , the “Super-weak” phase (assuming CPT)         |                     |                 |                 |                  |
|   | $\phi_{SW}$ result  | stat. error     | syst. error     | total error      |
| E731 $\pi^+\pi^-$ data<br>(preliminary)                                 | $43.37^\circ$       |                 |                 | $\pm 0.22^\circ$ |
| PDG average   | $43.51^\circ$       |                 |                 | $\pm 0.14^\circ$ |
| D. Fits for $\Delta\phi = \phi_{00} - \phi_{+-}$                        |                     |                 |                 |                  |
|   | $\Delta\phi$ result | stat. error     | syst. error     | total error      |
| E731 full data set<br>(preliminary)                                     | $-0.6^\circ$        | $\pm 1.4^\circ$ | $\pm 0.8^\circ$ | $\pm 1.6^\circ$  |
| NA31 '87 <sup>17)</sup>   | $+0.2^\circ$        | $\pm 2.6^\circ$ | $\pm 1.2^\circ$ | $\pm 2.9^\circ$  |
| E731 (20% data) <sup>18)</sup>  | $-0.3^\circ$        | $\pm 2.4^\circ$ | $\pm 1.2^\circ$ | $\pm 2.7^\circ$  |

| E. Fits for $\phi_{+-}$ (assumes analyticity for $\phi_\rho$ ) |                    |                 |                 |                 |
|--|--------------------|-----------------|-----------------|-----------------|
|  | $\phi_{+-}$ result | stat. error     | syst. error     | total error     |
| E731 $\pi^+\pi^-$ data<br>(preliminary)                        | 43.2°              | $\pm 1.3^\circ$ | $\pm 0.8^\circ$ | $\pm 1.6^\circ$ |
| PDG  | 46.0°              |                 |                 | $\pm 1.2^\circ$ |

## CONCLUSIONS

In conclusion, the E731 preliminary result (full data sample) is  $Re(\epsilon'/\epsilon) = (6.0 \pm 6.9) \times 10^{-4}$ , which is consistent with zero, in conflict with the NA31's non-zero result,  $Re(\epsilon'/\epsilon) = (23 \pm 7) \times 10^{-4}$ . The two results only differ by 1.7 sigma, but the probability that the two experiments are compatible is less than 10%. Although the two experiments have reached similar precision (better than  $10^{-3}$ ), one is dominated by the systematic uncertainty (NA31) and the other is limited by the statistics (E731). Measurements on  $\tau_S$  and  $\Delta m$  from E731's data in the  $2\pi$  system give good agreement with the previous measurements. The results on  $\Delta\phi$ ,  $\phi_{+-}$  and  $\phi_{SW}$  strongly support the CPT invariance.

The Standard Model generally predicts a non-zero result of order  $10^{-3}$ , but there are large uncertainties and possible cancelation effects. Although the Standard Model may be able to accommodate very small  $\epsilon'/\epsilon$ , (if the top quark mass is very heavy, say  $m_t > 220$  GeV), the theoretical uncertainties in the hadronic matrix elements must be reduced for the experimental results on  $\epsilon'/\epsilon$  to be used as a constraint.

The  $\epsilon'/\epsilon$  results have led both groups to propose new round experiments to measure the  $\epsilon'/\epsilon$  to a better precision at  $1 \times 10^{-4}$  in the near future.

The new experiment of the E731 group, called E832, will use the same technique of simultaneous  $K_S$  and  $K_L$  beams and will record all four decay modes at the same time, as in the 20% data sample. They

will very likely use pure CsI crystals for the electromagnetic detector to have better than 1% energy resolution for photons.

The new proposal of the NA31 group, called NA48, has the following new features:

(1) They will now use simultaneous  $K_S$  and  $K_L$  beams. They plan to tag interactions in a close target to signal a  $K_S$  candidate. All four modes will be taken simultaneously this time.

(2) They will not move the  $K_S$  with respect to the  $K_L$ .

(3) They will now use the magnetic spectrometer to reconstruct the charged decays, instead of using the purely calorimetric technique.

(4) They will use pure liquid Krypton for their electromagnetic detector and a tower geometry for the photon detection to get ~1% energy resolution.

Both experiments are planning to run in 1994, if the funding agencies, lab directors and program committees are willing to support the new detectors.

## REFERENCES

- 
1. J. H. Christenson, J. W. Cronin, V. L. Fitch, and R. Turlay, *Phys. Rev. Lett.* **13**, 138 (1964).
  2. M. Kobayashi and T. Maskawa, *Prog. Theor. Phys.* **49**, 659 (1973).
  3. L. Wolfenstein, *Phys. Rev. Lett.* **13**, 562 (1964).
  4. G. Buchalla, A.J. Buras, and M.K. Harlander, *Nucl. Phys.* **B337**, 313 (1990); J.M. Flynn and L. Randall, *Phys. Lett.* **B244**, 221 (1989).
  5. T.J. Devlin and J.O. Dickey, *Rev. Mod. Phys.* **51**, 237 (1979).

- 
6. H. Burkhardt *et al.*, *Phys. Lett.* **B206**, 169 (1988).
  7. J.R. Patterson *et al.*, *Phys. Rev. Lett.* **64**, 1491 (1990).
  8. G. Buchalla, A.J. Buras, and M.K. Harlander, MPI-PAE-Pth-30/90, July, 1990.
  9. J.F. Donoghue *et al.*, *Phys. Reports* **131**, 320 (1986).
  10. G. Barr (NA31 Collaboration), to appear in the *Proceedings of the Lepton Photon Conference*, Geneva, Switzerland, August 1991.
  11. B. Winstein (E731 Collaboration), to appear in the *Proceedings of the Lepton Photon Conference*, Geneva, Switzerland, August 1991.
  12. See, for example, J. Roehrig *et al.*, *Phys. Rev. Lett.* **38**, 1116 (1977).
  13. A. Gsponer *et al.*, *Phys. Rev. Lett.* **42**, 13 (1979); also, R.H. Bernstein *et al.*, *Phys. Rev. Lett.* **54**, 1631 (1985); M. Woods *et al.*, *Phys. Rev. Lett.* **60**, 1695 (1988).
  14. W.C. Carithers, *et al.*, *Phys. Rev. Lett.* **34**, 1244 (1975).
  15. Particle Data Group, *Review of Particle Properties*, *Phys. Lett.* **B239**, (1990).
  16. C. Gewniger, *et al.*, *Phys. Lett.* **B52**, 108 (1974).
  17. R. Carosi *et al.*, *Phys. Lett.* **B237**, 303 (1990).
  18. M. Karlsson *et al.*, *Phys. Rev. Lett.* **64**, 2976 (1990).